Characterizing the state and processes of change in a dynamic forest environment using hierarchical spatio-temporal segmentation

Authors:
Cristina Gómez[1], Joanne C. White[2], Michael A. Wulder[2*]

Affiliations:

[1]Sustainable Forest Management Research Institute, ETS de Ingenierías Agrarias, Universidad de Valladolid, Palencia, 34004, Spain

[2]Canadian Forest Service (Pacific Forestry Centre), Natural Resources Canada, Victoria, British Columbia, V8Z 1M5, Canada

*Corresponding author:
Mike Wulder
Phone: 250-363-6090; Fax: 250-363-0775; Email: mike.wulder@nrcan.gc.ca

Pre-print of published version.

Reference:
Gómez, C., J.C. White, and M.A. Wulder. (2011). Characterizing the state and processes of change in a dynamic forest environment using hierarchical spatio-temporal segmentation. Remote Sensing of Environment. Vol. 114, No. 7, pp. 1665-1679.

DOI.
http://dx.doi.org/10.1016/j.rse.2011.02.025

Key words: Landsat, spectral trajectory, Tasseled Cap Angle, TCA, Process Indicator, PI, forest, change, hierarchical spatio-temporal segmentation, monitoring, landscape pattern, landscape process

Abstract

Discrete changes in forest abundance, distribution, and productivity are readily detectable using a number of remotely sensed data sources; however, continuous changes such as growth and succession processes are more difficult to monitor. In this research we explore the potential of spectral trajectories generated from a 35-year (1973–2008) time-series of Landsat imagery to characterize change processes in a dynamic forest environment in northwestern Alberta, Canada. We propose a method of hierarchical spatio-temporal segmentation that enables the characterization of change processes that are spatially diffuse and temporally imprecise. Calibrated imagery from Landsat sensors are radiometrically normalized and two metrics derived from the Tasseled Cap Transformation components, greenness and brightness, are used to generate the Tasseled Cap Angle (TCA). The TCA is a measure of the proportion of vegetation to non-vegetation (the occupation state), and its derivative, the Process Indicator (PI), is a measure of change in this proportion through time. These indices condense information from the visible and near-infrared wavelengths, and facilitate lengthy time series analysis of forest landscape change using data from all Landsat sensors.

A combination of the original TCA and its derivative sequence are input to a three level hierarchical segmentation process with the highest and lowest levels defining homogeneous objects at the initial and final date, and the intermediate level identifying trajectories with similar change processes. The development through time of the TCA and PI are described, and the spatial and temporal associations of processes are statistically assessed using the Moran's Index.

A full range of change types were identified on the landscape, from stand replacing disturbances to more subtle growth and succession processes. Results indicate that the study area is in a constant state of change, and maintains a high average proportion of vegetation to non-vegetation. The amount of total landscape modified per decade increased from 18% and 14% in the 1970s and 1980s respectively, to more than 30% and 33% in the 1990s and 2000s. On average, the proportion of vegetation to non-vegetation was increasing prior to 1981, decreasing between 1981 and 1997, and increasing post-1997. There was a high degree of spatial autocorrelation amongst change processes, with a maximum Moran's I of 0.79 in 1973; landscape change became more spatially disperse and widespread after 1981. Temporal correlation of change processes was observed locally, with the period 1990-1995 having the most persistent change.

Introduction

Forests are naturally dynamic ecosystems in continuous change with a key role in water (Van Dijk and Bruijnzeel, 2001) and carbon cycles (Muukkonen and Heiskanen, 2007), and in wildlife habitat quality (Nadkarni et al., 2004). Ecological benefits provided by forests depend on the stage of development, health condition, spatial distribution, and structural characteristics (Spies et al., 1994; Wulder et al., 2008a; Numa et al., 2009). The ecological and economic services delivered by forests are markedly altered after disturbances such as fire or harvest, and are more steadily modified when subtle growth, natural succession, or decay occur.

Insights into patterns, rates, and trends of landscape changes are necessary to understand forest dynamics, enable preservation, and assess the effectiveness of management approaches (Hayes & Cohen, 2007; Huang et al., 2009a). Remotely sensed data have become a major information source for change detection (Lu et al., 2004) and are possibly the only feasible and cost-effective option for extensive areas (Lunetta et al., 2004). The Landsat series of satellites, the first of which was launched in 1972, provides a lengthy temporal sequence of images, and is unique among Earth observing satellites with imagery systematically collected to ensure global coverage, processed to an end-user applications ready state, and available via the Internet without cost. The spatial resolution (30 m), revisit cycle (16 days), and spatial extent (185 km x 185 km) of Landsat data are well suited to characterizing forest change (Wulder et al., 2008b).

Our goal is to explore the capacity of spectral trajectories generated from a 35-year time-series of Landsat images for exploration and analysis of spatially and temporally diffuse change in a dynamic forest environment. For this purpose we develop a *hierarchical spatio-temporal segmentation* method that combines information at various spatial and temporal resolutions; the persistence of relations between objects at the multilevel scale is assured by its hierarchical character. Specific objectives of this study are:

1. To characterize forest landscape change using an index generated from the Tasseled Cap Transformation components Greenness and Brightness, as well as the first derivative of this index. This index characterizes the proportion of vegetation to non-vegetation in a pixel and uses spectral channels that enable bridging across all Landsat sensors.
2. To incorporate both spatial and temporal properties into a hierarchical segmentation process to capture landscape-level change and incorporate spatial information regarding these change units through time.
3. To analyze the spatial and temporal correlations of changes through time over an area with changing amounts, rates, and related spatial distributions of disturbance in a study area important from both ecological (habitat) and economic perspectives.

Background

1.1 Disturbances and subtle change

Abundant research effort has focused on the assessment of disturbances in large area monitoring programs. Stand replacing disturbances, such as clearcuts and wildfires that drastically modify the landscape and require a lengthy period of time to recover their initial state, can be detected with confidence using remotely sensed data (Coops et al., 2006), particularly Landsat data. For example, Cohen et al. (1998) applied and compared various methods for mapping clearcuts in Western Oregon, achieving results with greater than 90% accuracy. In the same region, Cohen et al. (2002) characterized the rate and distribution of stand replacing disturbance over a 23-year period with MSS and TM images, finding public land more affected by natural disturbance, while private land was more intensely harvested. Healey et al. (2005) compared the ability of four Tasseled Cap (TC) structures in detecting harvest disturbance; a newly developed Disturbance Index (DI) was the best performer in areas with slower succession rates. The DI was later used by Masek et al. (2008) to compile a 10-year record of forest disturbances in North America, reporting omission errors of 30-60% and commission errors of 20-30%.

Less studied is the characterization of subtle, slow, continuous change related to partial harvest and natural regeneration or decay processes, which have less obvious effects on the landscape (Coops et al., 2006). Forest successional stages have been described (Cohen et al., 1995; Jakubauskas, 1996; Helmer et al., 2000), but studying the transitions between development stages is less common: Peterson and Nilson (1993) described trajectories of reflectance change in secondary succession of mono- specific birch and pine stands in Estonia; Schroeder et al. (2007) characterized patterns of recovery post-harvest in Western Oregon, and Vogelmann et al. (2009) characterized forest decline and mortality caused by persistent insect defoliation from 1988 to 2006 in New Mexico.

1.2 Time series of images and spectral trajectory

Two images acquired at different dates may be sufficient for identifying landscape change (Coppin & Bauer, 1996); however, the use of more than two image dates is recognized as a superior technique when the objective is to characterize the rate of change (as opposed to just the presence or absence of change) (Goodwin et al., 2008). A time series of remotely sensed images enables the identification of a greater range of processes (Gillanders et al., 2008) as well as the characterization of temporal patterns. Dense time-series are particularly useful for detecting change in very dynamic forests with a fast recovery rate (Huang et al., 2009b; Lunetta et al., 2004). Interpretation of a sequence of images, or temporal trajectory, makes it possible to characterize vegetation dynamics on different temporal scales (Bontemps et al., 2008). With the extensive Landsat image archive of the USGS being made freely available to the public (Woodcock et al., 2008) it has become possible to obtain a considerable number of images for long-term monitoring of ecosystems and for trajectory analysis approaches (Linke et al., 2009).

1.3 Object analysis approach for change detection

Object-based analysis has increased in the Earth Observation community in the last decade (Hay et al., 2005; Blaschke, 2010) as an alternative to pixel based analysis. Among the strengths of object-based analysis for change detection are the reduction of misregistration and shadowing effects (Johansen et al., 2010) and the inclusion of contextual information.

The spatial resolution of the imagery selected is crucial in the definition of objects analogous to forest stands. Landsat medium spatial resolution is well suited to the detection of change in forest environments at the stand level. The study of change with an object approach, and particularly the definition of objects can be done in a number of ways: if using various images, the segments can first be defined on a reference image and compared later in other dates (Hall and Hay, 2003); alternatively, objects could be defined by a pre-existing GIS layer as in Walter (2004); a third approach is the simultaneous segmentation of various dates of images (Desclée et al., 2006; Bontemps et al., 2008).

Methods

1.4 Study area

The study area covers 13,818 km^2 of the Foothills boreal forest region (Rowe, 1972) on the eastern side of the Rocky Mountains, Alberta, Canada (Figure 1). It is a transition zone between boreal and sub-alpine forest regions with lodgepole pine (*Pinus contorta* Dougl.ex Loudon), trembling aspen (*Populus tremuloides* Michx), and balsam poplar (*Populus balsamifera* L.) as prevalent pioneer tree species appearing after catastrophic events. Other species normally found in older stands are white spruce (*Picea glauca* (Moench) Voss) and black spruce (*Picea mariana* (Mill.) BSP) and less frequently white birch (*Betula papyrifera* Marsh.), tamarack (*Larix laricina* (Du Roi) K. Kock), balsam fir (*Abies balsamea* (L.)) and alpine fir (*Abies lasiocarpa* (Hook.) Nutt.). Elevation ranges from 600 to 2500 m.

The area is rich in live and fossilized natural resources (Alberta Sustainable Resource Development, 2009) and provides important habitat for grizzly bear (*Ursus arctos* L.) (Nielsen et al., 2004) and woodland caribou (*Rangifer tarandus caribou* Gmelin). Industrial extraction activities such as oil and gas, mining, and forest harvesting have been ongoing since the 1950s (Andison, 1998), with an increased intensity in recent decades (Schneider et al., 2003).

<Insert Figure 1 around here>

1.5 Data

We used a time sequence of fourteen images (Table 1) acquired between 1973 and 2008 by the Landsat series of satellites with various sensors: the Multi-Spectral Scanner (MSS), the Thematic Mapper (TM), and the Enhanced Thematic Mapper Plus (ETM+). All images were selected within the summer and early fall seasons for consistency in forest phenological condition (Wulder et al., 2004). Images were obtained from the United States Geological Survey (USGS), the Global Land Cover Facility (GLCF), and the Canada Centre for Remote Sensing (CCRS) archives.

<Insert Table 1 around here>

1.6 Image Preprocessing

Preprocessing of a sequence of images for change detection has two critical stages: spatial registration to assure positional coincidence of features, and radiometric calibration and normalization to ensure changes in spectral reflectance correspond to actual change events. Failure to correctly perform either of these two could trigger significant errors in the analysis and lead to misinterpretation of change events (Lu et al., 2004).

All but two of the images were acquired in an orthocorrected format. The two images received in raw format were geometrically corrected using Toutin's model (PCI Geomatica) and registered to the 1995 TM base image using 250 Ground Control Points (GCPs) and the thin plate spline algorithm. All of the MSS images were resampled from their original 57 m spatial resolution to 30 m. Finally, an image-to-image registration was used to co-register all of the images to the base image with a RMS error of less than 30 m (1 pixel).

Robust radiometric preprocessing is essential for monitoring landscape change (Lu et al., 2004) and for linking images with biophysical phenomena (Gong and Xu, 2003); it is particularly challenging if images from various sensors are included in the analysis (Roder et al., 2005). We used the approach of Han et al. (2007) to convert digital numbers to Top of Atmosphere (TOA) radiance with coefficients recommended by Chander et al. (2009). Greenness and Brightness components of the Tasseled Cap Transformation (TCT) (Kauth and Thomas, 1976; Crist and Cicone, 1984; Huang et al., 2002) were calculated and normalized to the reference image Greenness and Brightness, as in Powell et al., (2008). For relative radiometric normalization we applied IR-MAD (Iteratively Reweighted Multivariate Alteration Detection) (Canty et al., 2004) as recommended by Schroeder et al., (2006) for temporal spectral trajectories. This automatic process is based on the invariance property of MAD transformation and performs an orthogonal linear regression (Canty and Nielsen, 2008) of the target image pixels on to the reference image pixels; the process is invariant to linear transformations (Nielsen et al., 1998; Canty et al., 2004). The reference was a Landsat-5 TM image free of clouds and haze, dated 1995, in the middle of the series. The process of normalization reduces the amount of artifacts due to illumination or atmospheric variations, enabling more reliable detection of true change (Song et al., 2001).

1.7 Tasseled Cap Angle (TCA)

The Tasseled Cap Transformation (TCT) (Kauth and Thomas, 1976; Crist and Cicone, 1984; Crist, 1985; Huang et al., 2002) is a linear transform of the original Landsat spectral space that has been broadly employed in forestry applications (Cohen and Goward, 2004). It has served to characterize forest structure (Hansen *et al*. 2001; Cohen et al., 2002), condition (Wulder et al., 2006; Healey et al., 2006), successional state (Peterson *et al.* 1993, Helmer *et al.* 2000), and also for change detection (Lea *et al*. 2004, Jin and Sader 2005). The first two orthogonal components of the TCT, Brightness (B) and Greenness (G) define the *vegetation plane* (Crist and Cicone, 1984) (Figure 2, a) and are a practical bridge between MSS and TM-ETM+ imagery (Powell et al., 2008).

The study of forest stands' spectral behavior in the *vegetation plane* provides insights into forest cover densities (Cohen et al., 1995; Cohen et al., 1998) and forest development stages (Peterson and Nilson, 1993; Price and Jakubauskas, 1998). The B component is by definition a positive value, whereas G depends on the contrast between the visible and near-infrared bands

(Table 2), with exposed soil having negative values (Gillanders et al., 2008) and vegetated areas having positive values.

<Insert table 2 around here>

The Tasseled Cap Angle (TCA), defined as the angle formed by G and B in the vegetation plane (equation 1), condenses in a single value the information of the relation G/B (Figure 2, a) and represents essentially the proportion of vegetation to non-vegetation. A range of studies in coniferous forests have confirmed higher values of G and lower values of B in dense cover classes when compared to open stands or clearcuts (Cohen *et al*. 1995, Price and Jakubauskas, 1998). Accordingly, dense forest stands show higher TCA values than more open stands or bare soil (Figure 2, a). We evaluated the TCA in the study area, assessing values over a set of 5000 stand replacement disturbance events dated between 1972-2008, finding TCA in recent clearcuts significantly lower than in any other cover stage of the forest and a clear increasing tendency with time-since-disturbance (Figure 2, b).

$$TCA = arctan\ (G/B) \tag{1}$$

<Insert Figure 2 around here>

The range of values of the TCA is scene dependent, as are the TCT components (Crist and Cicone, 1984). An absolute assessment of forest density with the TCA would require local calibration with field data. On the contrary, evaluating relative changes of TCA does not require calibration: increments or reductions in the proportion of vegetation to non vegetation results in a concomitant change of TCA values.

The TCA images for each date were combined into a single, multi-band image file, hereafter called *TCA image* for further analysis. To describe the forest landscape cover with the TCA we define the *occupation state* characterizing categories of proportion of vegetation to non-vegetation: areas more densely occupied by vegetation have higher values of TCA than areas with less dense vegetation; the bare soil situation, with zero proportion of vegetation is illustrated with negative values of the TCA.

1.8 Image Masks

To reduce the detection of false changes, we excluded areas with elevations greater than 1700 m, water bodies, clouds and cloud shadows prior to analysis. High elevation areas were identified with a digital elevation model, water bodies were identified with 1:50,000 National Hydrology Network data; clouds and cloud shadows were identified using a semi-automatic approach for each image. The area remaining for analysis, after all masks were applied to the *TCA image*, was approximately 12,740 km^2.

1.9 Process Indicator (PI): the TCA derivative

The spectral profile of the *TCA image* at each pixel characterizes the evolution or trajectory of its TCA value over time. Each pixel trajectory was approximated with a Lagrange second order polynomial (Appendix A), which enables interpolation with uneven intervals among occurrences.

The interpolated TCA image was derived with respect to time (years), producing a new cube with the same number of bands as the TCA image, hereafter called *Process Indicator* (PI) *image*, where each pixel's spectral profile is the derivative of its corresponding input image's profile (Figure 3). Values of this new image represent the rate of TCA change over time, and unlike image difference methods, this technique assigns a value to each input date. The PI profile is the derivative of a smoothed curve, and is appropriate for detecting continuous subtle changes such as natural succession and decay, and progressive decadence due to disease or insect attack, which are difficult to assess with traditional change detection techniques (Coops et al., 2006).

<Insert Figure 3 around here>

1.10 Hierarchical spatio-temporal segmentation

Image segmentation is the partitioning of an image into homogeneous spatial units (Devereux et al., 2004) based on one or more attributes to facilitate visualization and analysis of spatially correlated properties; basic subdivisions contain information about raster attributes, shape, and position. *Hierarchical spatio-temporal segmentation* is a technique for exploration and analysis of changing properties of the landscape at various spatial and temporal scales: an image is divided in a hierarchy of levels, each one inheriting or passing on the boundaries of its objects to the subsequent level. The attributes of the spatial units, e.g. the spectral trajectory can be analyzed. The underlying assumption is that forest *change processes* are spatially and temporally correlated at certain scales.

There is no unique and singular solution to how an image partitions the landscape (Burnett and Blaschke, 2003) for ecological analysis and no single spatial scale is optimal for characterizing the multiple options in which the image can be divided (Hay et al, 2005). Attempting to interpret processes with a multi-scale segmentation requires the definition of semantic rules to relate lower level landscape units to higher levels of organization (Burnett and Blaschke, 2003). Three is the minimum number of levels recommended for landscape analysis (O'Neill, 1986).

The current landscape in the study area is highly fragmented as a result of natural factors and human activities (Andison 1998), and spatial units at the same *occupation state* are smaller than a few decades ago. We define two levels of segmentation based on initial (1973) and final (2008) TCA values (L3 and L1 respectively). The smaller objects in L1 made up larger homogeneous spatial units at the beginning of the period considered; each of them has evolved following a different process path. An intermediate *process level* (L2) defined by the *PI* trajectory (*change process*) links both *state levels* (Figure 4).

<Insert Figure 4 around here>

We introduce a mixed top-down/bottom-up approach whereby information at higher levels of the segmentation hierarchy (top: larger objects) is used to derive information at lower levels of the segmentation hierarchy (bottom: smaller objects) and vice versa (Hay et al., 2001). The order followed in the definition of objects in a hierarchical multi-scale segmentation of the landscape incorporating state and processes is important for interpretation and analysis. At the *state levels* L1 and L3, intra-object TCA variability is smaller that inter-object variability. The intermediate *process level* L2 acts as a bridge between the actual conditions (2008 TCA) and the initial state (1973 TCA), its segments have had similar changing path (PI trajectory) during the study period (1973-2008). Adjacent objects in level 2 followed a significantly different evolution path, and there is more variability in the process path between objects than within objects (Definiens, 2005).

The process of segmentation is performed with Definiens Cognition Network Technology® (Baatz and Schäpe, 2000; Definiens, 2005). L1 is defined with scale parameter 10, color-shape 0.7-0.3, smoothness-compactness 0.5-0.5 (Wulder and Seemann, 2003); the scale is 20 for L2 and 50 for L3. In defining the *process level* all PI layers are equally weighted.

1.11 Spatio-temporal correlation of forest occupation states and forest change processes

Once objects were defined, we sought to describe how *occupation states* and *change processes* were arranged across the study area within single years, and whether the condition of an object in one year was related to its condition and its neighborhoods' in a subsequent year. Thus, we required spatial statistics that could be calculated both at a local scale and a global scale, and could include both intra- and inter-year effects. We employed the Moran's Index (Moran, 1948) statistic (Appendix B) implemented in GeoDa™ which is free software dedicated to spatial data analysis (Anselin et al., 2006).

Moran's I can be interpreted as a spatially weighted form of Pearson's correlation coefficient (Goovaerts et al., 2005): positive and negative *z-values* point to positive and negative spatial correlation of objects' values respectively, and a zero value indicates there is no spatial association in the dataset. The *Moran scatterplot* facilitates visual exploration and interpretation of the global value of Moran's I (Anselin, 1993) (Figure 5): the distribution of the cloud of points (observation versus *spatial lag* (neighbor's weighted averaged values)) reflects the pattern of spatial association, and the slope of the regression line is an estimation of the global Moran's I.

<Insert Figure 5 around here>

For explicitly spatial description, local associations (clusters) and outliers can be identified and analyzed with a *Local Indicator of Spatial Analysis* (LISA) (Anselin, 1995). In this study we implemented the local Moran's I for detection of local patterns of forest *occupation state* and forest *change processes*, and created maps of clusters (*LISA cluster map*) that identify and classify (*high-high*, *low-low*, *high-low* and *low-high*) locations with significant association.

Spatial and temporal correlations of objects' TCA and PI values were assessed independently as a variable evaluated at multiple dates. LISA analysis of univariate data enables detection of spatial patterns of correlation at a single date. Furthermore, the option of bivariate LISA analysis facilitates temporal analysis of the spatial correlation, detecting if there is any association between the variable measured at a reference time and the same variable measured in the neighborhood at a different time (Anselin, 2003). In all our spatial analysis we defined the neighborhoods with the first order Queen's contiguity measure, i.e. each object's neighborhood consists of all other segments sharing some boundary with it.

Results

1.12 Hierarchical spatio-temporal segmentation

The hierarchical spatio-temporal segmentation yielded a number of objects at each level of segmentation with the average size per object shown in Table 3. There are 4.46 L2 objects per each L3 object on average, and 3.27 L1 objects in each L2 object on average. The average size of the smaller objects (L1) is approximately 40 ha.

<Insert Table 3 around here>

Most of the statistical summaries and results shown in following sections concern L1 objects; results at other levels of segmentation show similar trends.

1.13 Landscape occupation state--TCA

Considering the entire study area, the mean value of the objects' TCA is consistently greater than 190 over the whole period of analysis, and describes a landscape with a high proportion of vegetation to non-vegetation. Between 1997 and 2001, the mean TCA was at its lowest, with the minimum mean TCA occurring in 1997 (minimum average TCA value, Table 4, Figure 6) – the coincidence of three consecutive late season images in this period encourages a cautious interpretation. After 2001, TCA values trend upwards, indicating a global average increase in the proportion of vegetation to non-vegetation.

The standard deviation of the TCA (Figure 6, Table 4) indicates that the lowest dispersion in objects' TCA values occurred before 1990—images from the MSS era, with 6-bit rather than the 8-bit radiometric resolution of later Landsat sensors encourages cautious interpretation; since that time, the standard deviation has been higher, with a maximum in year 2001, which was the ceiling of diversity of *occupation states* at L1. As we would expect, from a high cover state, increased variance implies reduced cover, with non-vegetation locations (stand replacing disturbances) intermingled with forest stands at various stages of coverage and growth.

<Insert Table 4 around here>

<Insert Figure 6 around here>

The histograms of TCA distribution at all dates are similar, with a maximum occurring between values 220 and 240, but some differences are apparent (Figure 6). Of particular note is the variation, by year, of negative TCA values, indicative of non-vegetated areas, and of the high positive TCA objects that have a high proportion of vegetation or are densely occupied. To gain better insights of these changes, the range of TCA values over the scene was split in four categories, with a criterion based on the statistical distribution (the mean TCA, considering all dates, ± one standard deviation (i.e. 140, 310), and zero). Groups were labeled as *Negative* (TCA below zero, corresponding to non-vegetated objects), *Low, Medium,* and *High,* having an increasing proportion of vegetation to non-vegetation. Objects were classified in these four groups and their progression through TCA categories analyzed at a quasi-decadal interval: from 1973 to 1981; 1981-1990; 1990-2000; 2000-2008. Objects for which the TCA value changed category from initial to final date in each decade were counted (Figure 7).

<Insert Figure 7 around here>

In the 1970s, 17.8% of all L1 objects (5273) changed the *occupation state* enough to switch TCA category. Among these, 47% evolved from *medium* to *high* and 31% from *low* to *medium*: there was a clear net change towards higher densities and abundant interchange in the *high* and *medium* groups— areas with high coverage and also common change events inducing average TCA variations. In the 1980s, 13.8% of all L1 objects (4083) changed their *occupation state* sufficiently to switch TCA category. The *high* to *medium* and vice versa changes were again marked, with a net 11% change from *high* to *medium*. *Medium* to *low* changes accounted 29% of all changing objects; the overall change was towards lowering density. In the 1990s, 30.4% of all L1 objects (8989) switched the *occupation state* sufficiently to move TCA category, relating a transition over the landscape towards lower canopy cover densities: more than half of the changes in TCA category (56%) occurred from the *high* group to the *medium* group, followed by transition from *medium* to *low* (22%).

The last period analyzed, 2000-2008, experienced the highest rate of TCA category switches: 9972 L1 objects (33.7% of the total) swapped *occupation state* group. Among these, 60% exchanged from *medium* to *high*, 22% from *low* to *medium*, and 9% moved from *high* to *medium.* Despite the frequency of transformations produced in this time period, the global average *occupation state* was maintained (Figure 6).

We considered all mathematical options of transition amongst these TCA categories; in reality, however, frequent swaps at the spatial scale considered only occurred between adjacent groups, reflecting that changes of *occupation state* at the landscape level occur in a progressive manner. Transitions such as *high* to *negative*, *high* to *low,* or *negative* to *high* were infrequent or nonexistent in the study area at the time and spatial scale considered; such drastic changes would reveal alterations in *occupation state* produced by typical stand replacing disturbances such as fire, windthrow, or an accumulation of forest harvesting.

Summarizing change by decade is a useful approach, but sometimes a more detailed temporal examination is necessary for detecting trends. The total number of objects in each TCA category (Figure 7 left inset) reveals changing tendencies and aids in understanding fluctuations in the global average (Figure 6). TCA *medium* category objects are significantly more common than any other group between 1973 and 2008, oscillating between 67% and 84% of the total number of objects. The diminution of *high* objects between 1997 and 2001 is noteworthy and mathematically explains the decrease in the TCA global average (Figure 6). *Negative* and *low* categories of TCA are the least common objects for all dates, with a slight increment in *low* objects between 1997 and 2000; but late season images used to study this period (1997-2000) could somehow have conditioned lower values of the TCA.

1.14 Landscape change processes—PI

The average PI value describes the global state of change at the landscape level; assessing this average at consecutive dates (Figure 6) permits examination of trends in the study area. Prior to 1981, low positive values of the PI indicate a slow increasing rate in the proportion of vegetation to non-vegetation: the landscape is in an average state of forest growth. From 1981 to 1997, the average PI values are negative, indicating a decline in the proportion of vegetation to non-vegetation mainly caused by forest harvesting and, to a lesser extent, other disturbances; in the 2000s PI values are again positive (Table 4, Figure 6). The standard deviation of PI values (Table 4, Figure 6) is relatively high for the entire period indicating that this forest landscape is very dynamic and that there is a great variety of change processes occurring simultaneously.

Although the variation in the interval between image dates was considered when computing the PI values, the dearth of image data in the 1980s limits the analysis of trends. Further, the effect of late season imagery on PI values has to be considered in interpretation of changes. Despite these facts, a general decline in the *occupation state* (negative PI average) is observed in the 1980s and 1990s (Table 4, Figure 6) and a time of frequent and diverse change reflected by the high values of PI standard deviation.

For most image dates, the distribution of polygons with different *change processes* (PI values) is unimodal (Figure 6), with the majority of objects having a mean PI value close to zero (i.e., stable). The sample was divided in groups of PI values for exploration of changing patterns. With no ground truth to determine splitting thresholds, we used statistical criteria. The *stable* group, with PI close to zero, is a relevant group, representing areas with no change in the proportion of vegetation to non-vegetation. The *slow increase* and *slow decrease* groups were defined approximately by the values of the mean ± two standard deviations of PI at all dates (i.e., 60 and -70). The *fast increase* and *fast decrease* groups include the remaining extreme values (Figure 6).

Objects in the *fast decrease* group (i.e., being highly disturbed), are the smallest group in all time periods (Figure 8): there is a small proportion of the landscape with a rapid net loss of vegetation. Similarly, objects in the *fast increase* group (i.e., in a state of rapid emergence or occupation) are also relatively infrequent. In contrast, the *slow increment* PI objects (i.e., growing stands) are normally the most frequent, with the exception of 1995 and 1997, when *slow decrease* (i.e., decay by aging, disease, or partial harvest) was more common.

<Insert Figure 8 around here>

1.15 Spatial autocorrelation of forest occupation states and forest change processes

Global values of Moran's I show there is a consistent positive and high spatial autocorrelation of forest *occupation states* (TCA values) during the period from 1973 to 2008 (Table 5), with an average value of 0.643 at the L1 level of segmentation, and slightly lower for larger levels (results not shown). *Change processes* (PI values) are also positively and highly spatially correlated, with an average global Moran's I of 0.636 (Table 5). Whilst Moran's I values of TCA do not follow a clear trend, Moran's I values for PI generally decrease through time (Figure 9): similar *change processes* were spatially more concentrated at the beginning of the period of analysis, and have progressively lost spatial association, turning the landscape into a mosaic of *change processes* with smaller but more spread disturbance events and subsequent recovery. Observation of Figure

9 suggests there is no apparent correspondence between global spatial associations of TCA and PI values over time, state and process seem to have a different pattern.

<Insert Table 5 around here>

<Insert Figure 9 around here>

Exploration of the Moran's scatterplot informs about patterns of spatial autocorrelation, in particular if associations are between values over or below the average. As an example, the 1997 scatterplot of occupation states (TCA) (Figure 9, 1) illustrates that spatial associations at this date are produced between a large range of values below the average (Figure 9, Panel 1, Notation A). Spatial associations are also produced between values over, but close to the average (Figure 9, Panel 1, Notation B). In this case a few points in the upper left and lower right quadrants depict spatial outliers with markedly different occupation state compared to those neighboring; for instance these areas relate to changed areas (island polygons) amid unchanged forest areas (or the converse, unchanged islands amidst change).

The pattern of spatial association shown by the *Moran's scatterplot of change processes* (PI values) in 1973 is different, the distribution of points in both quadrants of positive correlation is similar (Figure 9, 2): there is spatial association between values below and over the average, i.e., processes of change are spatially associated, wether they are related with growth, disturbance or stabilization.

The temporal correlation of *occupation states* (TCA) and *change processes* (PI) is explored by studying the bivariate (temporal) Moran's I. The spatial association of the target variable at two consecutive dates is evaluated (Table 5) to investigate the impact of particular ocurrences on its neighborhood over time; care with different time intervals is necessary for interpretation. Results show global positive correlation of TCA at all time intervals (similar *occupation states* are spatially associated at consecutive dates, which seems very natural in the absence of disturbance), with a minimum of 0.352 in period 1976–1978 and a maximum of 0.656 in period 1978–1981. Bivariate (temporal) global Moran's I of PI is in most cases positive (Table 5) and not very large; a maximum of 0.494 occurs in period 2000-2001 and a minimum of -0.032 in period 1997–2000. The pattern of *Moran's scatterplot* of TCA (2000–2001 as an example in Figure 9, 3) is similar to the univariate case, with TCA values dispersed in the *low-low* quadrant and few outliers. In the PI example (1978–1981), the *temporal Moran's scatterplot* is an agglomeration of points around zero, different to the univariate case: while the univariate picture shows clustering of similar change processes, there is not a clear pattern of association in the bivariate case (Figure 9, 4) and areas at varying change processes of growth or decay at consecutive dates are intermingled.

Local analysis with a *map of clusters* can provide spatially explicit information on clustering (Figure 10) informing and characterizing local associations; it is a useful tool for visual interpretation. The examples in Figure 10 illustrate the association type of *change processes* (PI) in the study area for the period investigated (1973–2008). Red polygons denote association of values greater than average (*high-high*), blue polygons association of values less than average (*low-low*); purple polygons are *high-low* outliers (with a value greater than the mean at the initial date, and surrounded by polygons with values less than the mean at the second date) and green denotes *low-high* outliers (with a value less than the mean at the initial date, and surrounded by polygons with values greater than the mean at the second date). Polygons of the same type grouped together indicate larger homogeneous areas with respect to the variable analysed, as occurs in 1995–1997, whereas small groups of clusters or isolated patches indicate a more heterogeneous landscape, as is the case in 1978–1981.

Despite the low values of global Moran's I for temporal PI correlation (Table 5), local analysis and examination of the cluster maps reveal that there is a substantial number of *change process* clusters of all categories.

<Insert Figure 10 around here>

The varying time intervals between available image data makes inference of trends in temporal association less reliable; a periodic series of images would facilitate a thorough temporal study. To investigate a possible trend, we calculated global and local correlations at quasi-quinquennial intervals: 1976-1981, 1981-1990, 1990-1995, 1995-2000, and 2000-2006, and analysed total amounts of each category of local clusters (Table 6, Figure 10). Given the location (latitude and alpine transition) combined with local forest productivity levels influencing successioal processes, five to ten years is an adequate period to capture and portray the forest stand dynamics occuring; however, to detect more frequent changes, a complete series of annual images would be required.

<Insert Table 6 around here>

The highest number of significant ($p<0.001$) spatial clusters occur in the central periods, 1995-2000 and 2000-2005 (Figure 11, Table 6), a time with persistent change. It is between 1981-1990 when more positive spatial associations of change processes happens; interestingly, in this longer time lapse spatiotemporal associations are equally distributed between processes over the average (regrowth) and below the average (disturbance and decay) change process. A close look at the original images reveals that clearcutting practices and subsequent regrowth were more concentrated in fewer areas than during more recent dates. The time interval is an important parameter to control in the analysis of temporal correlation of *change processes* for accurate and reliable reports and conclusions, and although global values of correlation do not give exhaustive information, local analysis can give important and detailed spatial information.

<Insert Figure 11 around here>

Discussion

The Tasseled Cap derived indices employed in this work are valuable tools for the capture and assessment of forest cover condition and change. The *Tasseled Cap Angle* reports the proportion of vegetation to non-vegetation (*occupation state*) in a defined area and its derivative, the *Process Indicator* informs the current process of change. These indices condense information from the visible and NIR wavelengths, and facilitate comparison of data from all of the Landsat sensors, enabling the study of forest landscape change with a lengthy series of historical satellite images dating from 1973 to 2008. Results of our study indicate that the landscape change was more spatially clustered prior to 1981, but that change became more widespread and dispersed in later years. Certain periods had more intense change, as indicated by their temporal spatial correlation.

Forest landscapes, particularly managed forest landscapes, are dynamic ecosystems with a number of different change processes ongoing at any given time. Although a variety of remote sensing techniques have the capacity to detect stand replacing events, the detection of subtle alterations that result in only minor spectral changes remains a challenge (Goodwin et al., 2010) as different phenology and illumination of images induce detection of false change. With disrupting artifacts suppressed, the PI would be able to account for a wide variety of change types, providing information of slight or substantial modifications that is leveraged by a temporal series of three or more normalized images: low positive values of PI indicate a slow increment in the *occupation state* due to natural growth, while low negative values of PI point to natural processes of decay, such as aging or disease, or human induced modifications such as partial harvest or thinning (Table 7). More notable and fast changes in the *occupation state*, like a disturbance with reduction of vegetation or a process of vegetation emergence are indicated with high negative or positive values, respectively. The capacity to relate both positive and negative changes is a powerful aspect of the PI, enabling insights relating both forest (vegetation) gain and loss.

The TCA and PI, as derived from the TCT, are relative to the scene considered and would require a process of normalization to enable comparisons between different sites. If field data are not available, a study of relative change is the best option for the examination of trends. The availability of ground data for calibrating these indices could enable them to work as a look up table for other attributes, such as cover percentage, seral stage, or biomass content, facilitating forest monitoring efforts (e.g., Powell et al., 2010).

<Insert Table 7 around here>

Analyzing a temporal series of images supports the assessment of trends and rates of change that otherwise might be missed with only a bi-temporal change detection approach (Lunetta et al., 2004). The adequate interpretation of tendencies is conditioned by the time interval between consecutive images, and the scarcity of data for any one period may preclude a complete understanding of the landscape change. A decadal interval might be sufficient for preparing a summary of conditions and for planning silvicultural treatments and wood extractions, but more frequent information is required for monitoring of forest health and biomass. Jin and Sader (2005) recommend a period of three to five years for interpretation of condition and change in a forest area, but the ideal number of images and acquisition timing is site dependent (Wilson and Sader, 2002) and often restricted by image availability. We used a quasi-quinquennial interval for evaluation of change processes (PI) and a decadal interval for summary of change in the landscape state (TCA) obtaining sound and useful outcomes.

As long as temporal factors are considered, the interpretation of TCA and PI may be combined to provide insights on the *change processes* that are active in a forest landscape: varying rates of cover change could have different effects on dense or open forests and could trigger different phenomena. A simultaneous view of *occupation states* defining the landscape pattern and current *change processes* could help understanding the relation between pattern and process, a recursive question difficult to solve in landscape ecology (Turner, 1989; Walsh et al., 2009).

Although there is no confirmed link between these indices and ecological succession stages, the combined interpretation acts to facilitate analysis of succession patterns. The contextual temporal information given by the TCA enables proper interpretation of change that may be confounded with traditional techniques (Masek et al., 2008). The TCA provides information of vegetation proportion and the PI gives an instantaneous picture of the *change process*; together with some ecological knowledge, forest seral stages may be identified (i.e., young stand growing, young stand with disease, mature stand in decay, recovery from disturbance, or other situation). It must be noted that in order to enable accurate understanding of a trajectory of change, some knowledge of the local ecology is always required. Figure 12 depicts possible interpretation of consecutive *change processes* for a homogeneous area.

<Insert Figure 12 around here>

The object oriented approach implemented to help in the analysis of change at the landscape level provides meaningful reporting units, that is, objects analogous to forest stands. The spatial scale is a key parameter for assessment of ecological processes; we opted for a data driven method in the definition of spatial units, based on homogeneity of areas at the initial and final dates of the period (1973 and 2008). Establishing the hierarchy on the variables of interest, the transmission of significant information between levels is assured: initial and final state levels are connected through an intermediate level of processes accounting for the entire trajectory of change. Different intermediate levels could be defined for specific applications. For example, a forest health monitoring study may be interested in the progress of defined segments since the time of infection, and subtle changes could be detected from that point on. We reported the state and change of forest landscape with objects of a mean size of approximately 40 hectares, with a common initial state and intermediate history of change; however, the method allows any sized object to be used, enabling the selection of the most appropriate size given the ecological processes operating in the area.

Spatial and temporal autocorrelation is a complex and scale dependent phenomenon that is expected in natural environments. In the time period analyzed, some relations and patterns were unveiled for *occupation state* and *change processes.* The spatial correlation of *occupation state* was always positive; *change processes* were also positively correlated at the global spatial level and with a decreasing tendency over time. Temporal spatial autocorrelation of *change processes* was found in local aggregations, necessitating further analysis with local measure to understand the local variability.

Conclusion

The study of environmental long term historical change is facilitated with the free access to the United States Geological Survey Landsat data archive. Extensive areas can now be monitored retrospectively with techniques that incorporate multi-temporal information in a spatially explicit manner, and which are capable of seamlessly integrating data from a variety of sensors. An index derived from the well known TCT, the *Tasseled Cap Angle*, and its derivative, the *Process Indicator*, have demonstrated potential for characterizing the change in state and process in a dynamic forest area, enabling detection of subtle changes as well as more obvious stand-replacing disturbances. Combined, the interpretation of the TCA and its derivative, the PI, provides a simultaneous view of the occupation state and the change processes that are operating in a forest landscape, thereby enabling some understanding of the elusive relationships between landscape pattern and process—a recursive question of landscape ecology. A hierarchical segmentation process incorporating spatial and temporal properties provides flexibility in the establishment of the scale of analysis. Spatial statistics applied to multipixel objects enable assessment of spatial and temporal correlation of change events at the landscape level. Applications that require temporally detailed and spatially explicit information, such as forest succession studies, forest health monitoring, habitat models, and biomass or carbon accounting programs, will benefit from the use of these tools that provide dynamic information of the forest state and processes. Further work to link TCA and PI values with better known scales of forest variables is recommended to facilitate interpretation.

Acknowledgements

We acknowledge the Government Related Initiatives Program (GRIP) of the Canadian Space Agency (CSA) support of the project “EcoMonitor: Northern Ecosystem Climate Change Monitoring From Space” that enabled implementation of this research. The constructive comments of the anonymous reviewers are thanked for providing insightful, detailed, and helpful direction.

Appendix A. Lagrange interpolation of the TCA

The Lagrange interpolating polynomial of the TCA profile at each pixel is given by:

$$f_2(t) = \sum_{i=0}^{2} L_i(t)\, f(t_i) \tag{A1}$$

where $f_2(t)$ stands for the 2nd order polynomial that approximates the function $TCA = f(t)$ given at 3 data points as $(t_0, TCA_0), (t_1, TCA_1), (t_2, TCA_2)$, and the Lagrangian weights are:

$$L_i(t) = \prod_{\substack{j=0 \\ j \neq i}}^{n} \frac{t - t_j}{t_i - t_j} \tag{A2}$$

The polynomial formula for the interpolated TCA at each pixel is therefore:

$$TCA(t) = \left(\frac{t-t_1}{t_0-t_1}\right)\left(\frac{t-t_2}{t_0-t_2}\right)TCA(t_0) + \left(\frac{t-t_0}{t_1-t_0}\right)\left(\frac{t-t_2}{t_1-t_2}\right)TCA(t_1) + \left(\frac{t-t_0}{t_2-t_0}\right)\left(\frac{t-t_1}{t_2-t_1}\right)TCA(t_2) \quad t_0 \leq t \leq t_2 \tag{A3}$$

The PI or derivative of this polynomial can be expressed as:

$$PI(t) = \frac{2t - t_1 - t_2}{(t_0-t_1)(t_0-t_2)}TCA(t_0) + \frac{2t - t_0 - t_2}{(t_1-t_0)(t_1-t_2)}TCA(t_1) + \frac{2t - t_0 - t_1}{(t_2-t_0)(t_2-t_1)}TCA(t_2), \; t_0 \leq t \leq t_2 \tag{A4}$$

Appendix B. Moran's Index

Moran's Index can be expressed as:

$$I = \frac{N}{\sum_i \sum_j w_{ij}} * \frac{\sum_i \sum_j w_{ij}(x_i - \mu)(x_j - \mu)}{\sum_i (x_i - \mu)^2} \tag{A5}$$

Where x_i is the variable of interest x measured at location *i*, N the number of observations, μ the mean of the variable, and w_{ij} are the elements of the *spatial weights matrix*, which expresses the membership of observations in the neighborhood set for each location (Anselin, 1992).

A standardized *z-value* is reported for ease of interpretation.

$$z_i = \frac{I_i - E(I_i)}{\sqrt{V(I_i)}} \tag{A6}$$

References

Alberta Sustainable Resource Development, (2009). Annual Report 2008/2009. Alberta Resource Development, Edmonton, Alberta, Canada.

Andison, D.W. (1998). Temporal patterns of age-class distributions on foothills landscapes in Alberta. *Ecography* 21, 543-550

Anselin, L. (1992). Spatial data analysis with GIS: an introduction to application in the social sciences. Technical Report 92-10. National Center for Geographic Information and Analysis, University of California, Santa Barbara

Anselin, L. (1993). The Moran Scatterplot as an ESDA tool to assess local instability in spatial association. Research paper 9330. Regional Research Institute, West Virginia University and National Center for Geographic Information and Analysis, University of California, Santa Barbara.

Anselin, L. (1995). Local Indicators of spatial association-LISA. Geographical Analysis, 27, 93-115

Anselin, L. (2003). An introduction to spatial autocorrelation analysis with GeoDa. Spatial Analysis Laboratory, Department of Agricultural and Consumer Economics, University of Illinois, Urbana-Champaign, June 16, 2003

Anselin, L., Syabri, I., & Kho, Y. (2006). GeoDa: An Introduction to Spatial Data Analysis. *Geographical Analysis*, 38, 5-22

Baatz, M., & Schäpe, M. (2000). Multiresolution segmentation: An optimization approach for high quality multi-scale image segmentation. Proceedings of Angewandte Geographische Informationsverarbeitung XII. In J. Strobl, T. Blaschke, & G. Griesebner (Eds.), Beiträge zum AGIT Symposium (pp. 12−23). Salzburg 2000

Bontemps, S., Bogaert, P., Titeux, N., & Defourny, P. (2008). An object-based change detection method accounting for temporal dependences in time series with medium to coarse spatial resolution. *Remote Sensing of Environment*, 112, 3181-3191

Blaschke, T. (2010). Object based image analysis for remote sensing. *ISPRS Journal of Photogrammetry and Remote Sensing*, 65, 2-16

Burnett, C., & Blaschke, T. (2003). A multiscale segmentation object relationship modelling methodology for landscape analysis. *Ecological Modelling*, 168, 233-249

Canty, M.J., Nielsen, A.A., & Schmidt, M. (2004). Automatic radiometric normalization of multitemporal satellite imagery. *Remote Sensing of Environment*, 91, 441-451.

Canty, M.J., & Nielsen, A.A. (2008). Automatic radiometric normalization of multitemporal satellite imagery with the iteratively re-weighted MAD transformation. *Remote Sensing of Environment*, 112, 1025-1036.

Chander, G., Markham, B.L., & Helder, D.H. (2009). Summary of current radiometric calibration coefficients for Landsat MSS, TM, ETM+, and EO-1 ALI sensors. *Remote Sensing of Environment*, 113, 893-903

Cohen, W., Spies, T.A., & Fiorella, M. (1995). Estimating the age and structure of forests in a multi-ownership landscape of western Oregon, U.S.A. *International Journal of Remote Sensing*, 16 (4), 721-746

Cohen, W., Fiorella, M., Gray, J., Helmer, E., & Anderson, K. (1998). An efficient and accurate method for mapping forest clearcuts in the Pacific Northwest using Landsat imagery. *Photogrammetry Engineering & Remote Sensing*, 64 (4), 293-300

Cohen, W.B., Spies, T.A., Alig, R.A., Oetter, D.R., Maiersperger, T.K., & Fiorella, M. (2002). Characterizing 23 years (1972-95) of stand replacement disturbance in Western Oregon forests with Landsat imagery. *Ecosystems*, 5, 122-137

Cohen, W., & Goward, S. (2004). Landsat's role in ecological applications of remote sensing, *BioScience* 54, 535–545

Coops, N., M. Wulder, & J. White, 2006. Identifying and describing forest disturbance and spatial pattern: Data selection issues and methodological implications. Chapter 2 in: Wulder, M. and S. Franklin, (Editors), Forest Disturbance and Spatial Pattern: Remote Sensing and GIS Approaches, Taylor and Francis, Boca Raton, Florida, USA, 264p.

Coppin, P.R., & Bauer, M.E. (1996). Change Detection in Forest Ecosystems with Remote Sensing Digital Imagery. *Remote Sensing Reviews*, 13, 207-234

Crist, E. P., & Cicone, R. C. (1984). A physically based transformation of Thematic Mapper data-the TM tasseled Cap. *IEEE Transactions on Geoscience and Remote Sensing,* 22 (23), 256-263

Crist, E. P., (1985). A TM tasseled cap equivalent transformation for reflectance factor data. *Remote Sensing of Environment*, 17, 301-306.

Definiens. 2005. Definiens eCognition Version 5 Object Oriented Image Analysis User5 Guide, Definiens, AG, Munich, Germany.

Desclée, B., Bogaert, P., & Defourny, P. (2006). Forest change detection by statistical object based method. *Remote Sensing of Environment* 102, 1-11

Devereux, B.J., Amable, G.S., & Costa Posada, C. (2004). An efficient image segmentation algorithm for landscape analysis. *International Journal of Applied Earth Observation and Geoinformation*, 6, 47-61

Gillanders, S.N., Coops, N.C., Wulder, M.A., & Goodwin, N.R. (2008). Application of Landsat satellite imagery to monitor land-cover changes at the Athabasca Oil Sands, Alberta, Canada. *The Canadian Geographer*, 52 (4), 466-485

Gong, P., & Xu, B. (2003). Chapter 11: Remote Sensing of Forests over Time: Change Types, Methods, and Opportunities, Kluwer Academic Publishers, Dordrecht / Boston/ London. Remote Sensing of Forest Environments: Concepts and Case Studies

Goodwin, N.R., Coops, N.C., Wulder, M.A., Gillanders, S., Schroeder, T.A., & Nelson, T. (2008). Estimation of insect infestation dynamics using a temporal sequence of Landsat data. *Remote Sensing of Environment*, 112, 3680-3689

Goodwin, N.R., Magnussen, S., Coops, N.C., & Wulder, M.A. (2010). Curve fitting of time-series Landsat imagery for characterizing a mountain pine beetle infestation. *International Journal of Remote Sensing*, 31 (12), 3262-3271

Goovaerts, P., Jazquez, G.M., & Marcus, A. (2005). Geostatistical and local cluster analysis of high resolution hyperspectral imagery for detection of anomalies. *Remote Sensing of Environment*, 95, 351-367

Hall, O., & Hay, G. (2003). A multiscale object specific approach to digital change detection. *International Journal of Applied Earth Observation and Geoinformation*, 4, 311-327

Han, T., M. A. Wulder, J. C. White, N. C. Coops, M. F. Alvarez, & Butson, C. (2007). An efficient protocol to process Landsat images for change detection with Tasselled Cap Transformation. *IEEE Geoscience and Remote Sensing Letters*, 4 (1), 147-151

Hay,G.J., Marceau,D.J., Dubé, P., & Bouchard, A. (2001). A multiscale framework for landscape analysis: Object-specific analysis and upscaling. *Landscape Ecology*, 16, 471-490

Hay, G.J., Castilla, G., Wulder, M.A., & Ruiz, J.R. (2005). An automated object-based approach for the multiscale image segmentation of forest scenes. *International Journal of Applied Earth Observation and Geoinformation*, 7, 339-359

Hayes, D.J., & Cohen, W.B. (2007). Spatial, spectral and temporal patterns of tropical forest cover change as observed with multiple scales of optical satellite data. *Remote Sensing of Environment*, 106, 1-16

Healey, S.P., Cohen, W.B., Zhiqiang, Y., & Krankina, O. (2005). Comparison of Tasseled Cap-based Landsat data structures for use in forest disturbance detection. *Remote Sensing of Environment*, 97, 301-310

Healey, S.P., Yang, Z., Cohen, W.B., & Pierce, D.J. (2006). Application of two regression-based methods to estimate the effects of partial harvest on forest structure using Landsat data. *Remote Sensing of Environment*, 101, 115-126

Helmer, E.H., Brown, S., & Cohen, W. (2000). Mapping montane tropical successional stage and land use with multi-date Landsat imagery. International Journal of *Remote Sensing*, 21 (11), 2163-2183

Huang, C., Wylie, B., Yang, L., Homer, C., & Zylstra, G. (2002). Derivation of a tasselled cap transformation based on Landsat 7 at-satellite reflectance. *International Journal Remote Sensing*, 23(8), 1741-1748

Huang, Ch., Goward, S.N., Schleeweis, K, Thomas, N., Masek, J.G., & Zhu, Z. (2009a). Dynamics of national forests assessed using Landsat record: case studies in eastern United States. *Remote Sensing of Environment*, 113, 1430-1442

Huang, Ch., Goward, S.N., Masek, J.G., Gao, F., Vermote, E.F., Thomas, N., Schleeweis, K., Kennedy, R.E., Zhu, A., Eidenshink, J.C., & Tonwshend, J.R.G. (2009b). Development of time series stacks of Landsat images for reconstructing forest disturbance history. *International Journal of Digital Earth,* 1, 1-25

Jakubauskas, M.E. (1996). Thematic Mapper characterization of lodgepole pine seral stages in Yellowstone National Park, USA. *Remote Sensing of Environment*, 56, 118-132

Jin, S., & Sader, S.A. (2005). Comparison of time series tasseled cap wetness and the normalized difference moisture index in detecting forest disturbances. *Remote Sensing of Environment*, 94, 364-372

Johansen, K., Arroyo, L.A., Phinn, S., & Witte, C. (2010). Comparison of geo-object based and pixel-based change detection of riparian environments using high spatial resolution multi-spectral imagery. *Photogrammetric Engineering & Remote Sensing*, 76 (2), 123-136

Kauth, R.J., & Thomas, G.S. (1976). The tasseled cap --a graphic description of the spectral-temporal development of agricultural crops as seen in Landsat, in Proceedings on the Symposium on Machine Processing of Remotely Sensed Data, West Lafayette, Indiana, June 29 - July 1, 1976, (West Lafayette, Indiana: LARS, Purdue University), 41-51.

Linke, J., McDermid, G.J., Laskin, D.N., MacLane, A.J., & Hall-Beyer, M. (2009). A disturbance inventory framework for flexible and reliable landscape monitoring. *Photogrammetric Engineering & Remote Sensing*, 75 (8), 981-995

Lu, D., Mausel, P., Brondizio, E., & Moran, E. (2004). Change detection techniques. *International Journal of Remote Sensing*, 25 (12), 2365-2407

Lunetta, R., Johnson, D.M., Lyon, J., & Crotwell, J. (2004). Impacts of imagery temporal frequency on land-cover change detection monitoring. *Remote Sensing of Environment*, 89, 444–454

Masek, J.G., Huang, Ch., Wolfe, R., Cohen, W., Hall, F., Kutler, J., & Nelson, P. (2008). North American forest disturbance mapped from a decadal Landsat record. *Remote Sensing of Environment*, 112, 2914-2926

Moran, P.A.P. (1948). The interpretation of statistical maps. Journal of the Royal Statistical Society. Series B (Methodological), 10 (2), 243-251

Muukkonen, P., & Heiskanen, J. (2007). Biomass estimation over a large area based on standwise forest inventory data and ASTER and MODIS satellite data: A possibility to verify carbon inventories. *Remote Sensing of Environment*, 107, 617-624

Nadkarni, N.M., Parker, G.G., Rinker, H.B., & Jarzen, D.M. (2004). The nature of forest canopies. Chapter 1 in: Margaret D. Lowman & Nalini M. Nadkarni (Editors) Forest Canopies (Physiological Ecology). Elsevier Academic Press. 501 p

Nielsen, A.A., Conradsen, K., & Simpson, J.J. (1998). Multivariate Alteration Detection (MAD) and MAD postprocessing in multispectral, bitemporal image data: new approaches to change detection studies. *Remote Sensing of Environment*, 64, 1-19

Nielsen, S.E., Boyce, M.S., & Stenhouse, G.B. (2004). Grizzly bears and forestry I. Selection of clearcuts by grizzly bears in west-central Alberta, Canada. *Forest Ecology and Management*, 199, 51–65

Numa, C., Verdu, J.R., Sanchez, A., & Galante, E. (2009). Effects of landscape structure on the spatial distribution of Mediterranean dung beetle diversity. *Diversity and Distributions*, 15, 489-501

O'Neill, R.V., DeAngelis, D.L., Waide, J.B., & Allen, T.F. (1986). A Hierarchical Concept of Ecosystems. Princeton University Press, Princeton

Peterson, U. & Nilson, T. (1993). Successional reflectance trajectories in northern temperate forests. *International Journal Remote Sensing*, 14 (3), 609-613

Powell, S.L., Cohen, W.B., Yang, Z., Pierce, J.D., & Alberti, M. (2008). Quantification of impervious surface in the Snohomish Water Resources Inventory Area of Western Washington from 1972-2006. *Remote Sensing of Environment,* 112, 1895-1908

Powell, S.L., Cohen, W.B., Healey, S.P., Kennedy, R.E., Moisen, G.G, Pierce, K.B., & Ohmann, J.L. (2010). Quantification of live aboveground biomass dynamics with Landsat time-series and field inventory data: A comparison of empirical modeling approaches. *Remote Sensing of Environment,* 114, 1053-1068

Roder, A., Kuemmerle, T., & Hill, J. (2005). Extension of retrospective datasets using multiple sensors. An approach to radiometric intercalibration of Landsat TM and MSS data. *Remote Sensing of Environment*, 95, 195-210

Rowe, J.S. (1972). Forest regions of Canada. Canadian Forestry Service Department of the Environment, Otawa, Canada.

Schneider, R. R., J. B. Stelfox, S. Boutin, & Wasel, S. (2003). Managing the cumulative impacts of land uses in the Western Canadian Sedimentary Basin: a modeling approach. *Conservation Ecology,* 7(1), 8

Schroeder, T.A., Cohen, W.B., Song, C., Canty, M.J., & Yang, Z. (2006). Radiometric correction of multi-temporal Landsat data for characterization of early successional forest patterns in western Oregon. *Remote Sensing of Environment*, 103, 16-26

Schroeder, T.A., Cohen, W.B., & Zhiqiang, Y. (2007). Patterns of Forest regrowth following clearcutting in Western Oregon as determined from Landsat time-series. *Forest Ecology and Management*, 243, 259-273

Song, C., Woodcock, C.E., Seto, K.C., Lenney, M.P., & Macomber, S.A. (2001). Classification and change detection using Landsat data: when and how to correct atmospheric effects? *Remote Sensing of Environment*, 75, 230-244

Spies, T.A., Ripple, W.J., & Bradshaw, G.A. (1994). Dynamics and pattern of a managed coniferous forest landscape in Oregon. *Ecological Applications*, 4 (3), 555-568

Turner, M.G. (1989). Landscape ecology: the effect of pattern on process. Annual *Review of Ecology and Systematics*, 20, 171-197

Vogelmann, J.E., Tolk, B., & Zhu, Z. (2009). Monitoring forest changes in the southwestern United States using multitemporal Landsat data. *Remote Sensing of Environment*, 113, 1739-1748

Walsh, S.J., Brown, D.G., Geddes, C.A., Weiss, D.J., McKnight, S., Hammer, E.S., & Tuttle, J.P. (2009). Pattern-process relations in the alpine and subalpine environments: a remote sensing and GIScience perspective. Chapter 2 in: Elseveir Ed. Development in Earth Surface Processes, 12.

Wilson, E.H., & Sader, S.A. (2002). Detection of forest harvest type using multiple dates of Landsat TM imagery. *Remote Sensing of Environment*, 80, 385-396

Woodcock, C.E., Allen, R., Anderson, M., Belward, A., Bindschadler, R., Cohen, W., Gao, F., Goward, S.N., Helder, D., Helmer, E., Nemani, R., Oreopoulos, L., Schott, J., Thenkabail, P.S., Vermote, E.F., Vogelmann, J., Wulder, M.A., & Wynne, R. (2008). Free access to Landsat imagery. *Science*, 320, 5879, 1011

Wulder, M.A., & Seemann, D. (2003). Forest inventory height update through the integration of lidar data with segmented Landsat imagery. *Canadian Journal of Remote Sensing*, 29 (5), 536-543

Wulder, M.A., Franklin, S.E., & White, J.C. (2004). Sensitivity of hyperclustering and labeling land cover classes to Landsat image acquisition date. *International Journal Remote Sensing*, 10, 5337-5344

Wulder, M.A., White, J.C., Bentz, C., Alvarez, M.F., & Coops, N. (2006). Estimating the probability of mountain pine beetle red attack damage. *Remote Sensing of Environment*, 101 (2), 150-166

Wulder, M.A., White, J.C., Han, T., Coops, N.C., Cardille, J.A., Holland, T., & D. Grills. (2008a). Monitoring Canada forests. Part 2: National forest fragmentation and pattern. *Canadian Journal of Remote Sensing*, 34 (6), 563-584

Wulder, M.A., White, J.C., Goward, S.N., Masek, J.G., Irons, J.R., Herold, M., Cohen, W.B., Loveland, T.R., & Woodcock, C.E. (2008b). Landsat continuity: Issues and opportunities for land cover monitoring. *Remote Sensing of Environment*, 112, 955-969

Table 1. Landsat time-series of imagery used in the study

Landsat / Sensor	Path/Row	Date (dd/mm/yyyy)	Sun elevation (degrees)	Source
1 / MSS	50/22	16/09/1973	36.21	GLCF
2 / MSS	50/22	27/09/1976	30.40	CCRS
2 / MSS	50/22	25/07/1978	49.00	GLCF
2 / MSS	50/22	14/08/1981	46.10	CCRS
5 / TM	46/22	06/09/1990	37.38	USGS
5 / TM	46/22	23/07/1991	50.25	USGS
5 / TM	46/22	04/09/1995	36.99	USGS
5 / TM	46/22	25/09/1997	32.21	CCRS
7 / ETM+	46/22	25/09/2000	32.82	USGS
7 / ETM+	46/22	28/09/2001	31.70	USGS
7 / ETM+	46/22	15/09/2002	36.48	USGS
5 / TM	46/22	11/08/2004	47.31	CCRS
5 / TM	46/22	30/06/2006	55.86	USGS
5 / TM	46/22	06/08/2008	48.80	USGS

CCRS: Canadian Centre for Remote Sensing
GLCF: Global Land Cover Facility
USGS: United States Geological Survey

Table 2. Coefficients used for calculation of TCT indices

Sensor	Component	R	G	B	NIR	SWIR1	SWIR2
MSS	Brightness	0.433	0.632	0.586	0.264	N/A	N/A
	Greenness	-0.290	-0.562	0.600	0.491	N/A	N/A
TM	Brightness	0.3037	0.2793	0.4343	0.5585	0.5082	0.1863
	Greenness	-0.2848	-0.2435	-0.5436	0.7243	0.0840	-0.1800
ETM+	Brightness	0.3561	0.3972	0.3904	0.6966	0.2286	0.1596
	Greenness	-0.3344	-0.3544	-0.4556	0.6966	-0.0242	-0.2630

Table 3. Characteristics of hierarchical spatio-temporal segments

Level	Similarity	Attribute for definition	Mean Size (ha)	Number objects
L3	Initial *occupation state*	1973 TCA	634.4	2021
L2	*Change process* trajectory	1973-2008 PI	141.9	9032
L1	Final *occupation state*	2008 TCA	43.1	29544

Table 4. Statistics of TCA and PI values at L1 level

TCA	1973	1976	1978	1981	1990	1991	1995	1997	2000	2001	2002	2004	2006	2008
Mean	227.13	229.99	241.33	244.05	231.83	232.73	226.40	195.23	204.64	201.81	235.93	240.01	237.69	244.56
Std deviation	74.21	59.55	66.24	66.02	80.78	84.46	87.18	91.88	95.05	95.73	83.23	80.19	81.59	78.90
Kurtosis	5.57	2.14	5.55	6.30	4.58	10.03	8.62	10.74	15.34	13.48	7.43	7.96	8.30	8.89
Skewness	-1.21	-0.58	-0.86	-0.93	-1.21	-1.92	-1.99	-2.45	-2.98	-2.66	-1.67	-1.77	-1.75	-1.90
Min.	-463.92	-83.08	-450.94	-491.11	-322.71	-646.56	-505.43	-566.48	-735.87	-701.26	-457.65	-499.27	-539.34	-502.49
Max.	432.41	432.66	399.30	417.55	438.03	407.07	441.63	446.87	454.64	447.31	447.03	413.21	399.25	405.40
PI		**1976**	**1978**	**1981**	**1990**	**1991**	**1995**	**1997**	**2000**	**2001**	**2002**	**2004**	**2006**	
Mean		7.10	7.03	-4.75	-5.66	-2.71	-18.75	-10.88	3.29	15.64	19.10	0.88	2.27	
Std deviation		20.30	26.14	18.88	21.38	16.28	34.41	25.15	17.90	25.31	30.58	17.32	12.93	
Kurtosis		7.65	1.26	8.97	12.10	11.91	1.58	8.55	11.51	2.64	4.83	6.22	14.94	
Skewness		1.05	0.06	-1.07	-2.30	-1.21	-0.58	-1.21	-0.70	1.00	0.73	-0.12	-0.20	
Min.		-338.31	-227.89	-217.41	-320.04	-235.86	-310.10	-420.88	-369.72	-109.03	-213.48	-128.77	-126.84	
Max.		189.68	134.98	314.38	97.04	108.96	164.26	202.64	144.69	284.95	378.67	185.01	214.39	

Table 5. Values of Moran's Index of univariate (spatial) and bivariate (temporal) TCA and PI. All correlations with p-value<0.001

Spatial	**1973**	**1976**	**1978**	**1981**	**1990**	**1991**	**1995**	**1997**	**2000**	**2001**	**2002**	**2004**	**2006**	**2008**
TCA	0.6740	0.5397	0.6959	0.6709	0.6804	0.6813	0.6625	0.6083	0.5087	0.5983	0.6601	0.6723	0.6848	0.6657
PI	0.7940	0.6365	0.7275	0.6095	0.6690	0.6422	0.6880	0.6521	0.6311	0.6860	0.6070	0.5086	0.5691	0.5336

Temporal		**73-76**	**76-78**	**78-81**	**81-90**	**90-91**	**91-95**	**95-97**	**97-00**	**00-01**	**01-02**	**02-04**	**04-06**	**06-08**
TCA		0.3959	0.3523	0.6557	0.6003	0.6522	0.6290	0.5112	0.5637	0.5744	0.5284	0.6235	0.6448	0.6512
PI		0.1170	0.2259	0.0434	0.4209	0.1729	0.3140	0.4668	-0.0321	0.2301	0.4940	0.2360	0.1307	0.0397

Table 6. Number of significant PI ($p<0.01$) clusters for quasi-quinquennial intervals

Cluster	**1976-1981**	**1981-1990**	**1990-1995**	**1995-2000**	**2000-2006**
High-high	612	1559	1448	890	1192
Low-low	501	1239	885	561	370
Total positive	*1113*	*2798*	*2333*	*1451*	*1562*
High-low	1273	349	1788	2411	1205
Low-high	1015	306	2023	2393	1280
Total outliers	*2288*	*655*	*3811*	*4804*	*2485*
Total	3401	3453	6144	6255	4047

Table 7. Interpretation of TCA and PI values

Value		**TCA** *Occupation state*	**PI** *Change process*
Positive	High	High proportion Veg-nonVeg	Emergence
	Low	Low proportion Veg-nonVeg	Growth
Zero		Greenness = 0	Stable
Negative	Low	Non-vegetated	Decrease (natural decay or partial harvest)
	High	Non-vegetated	Disturbance

FIGURES

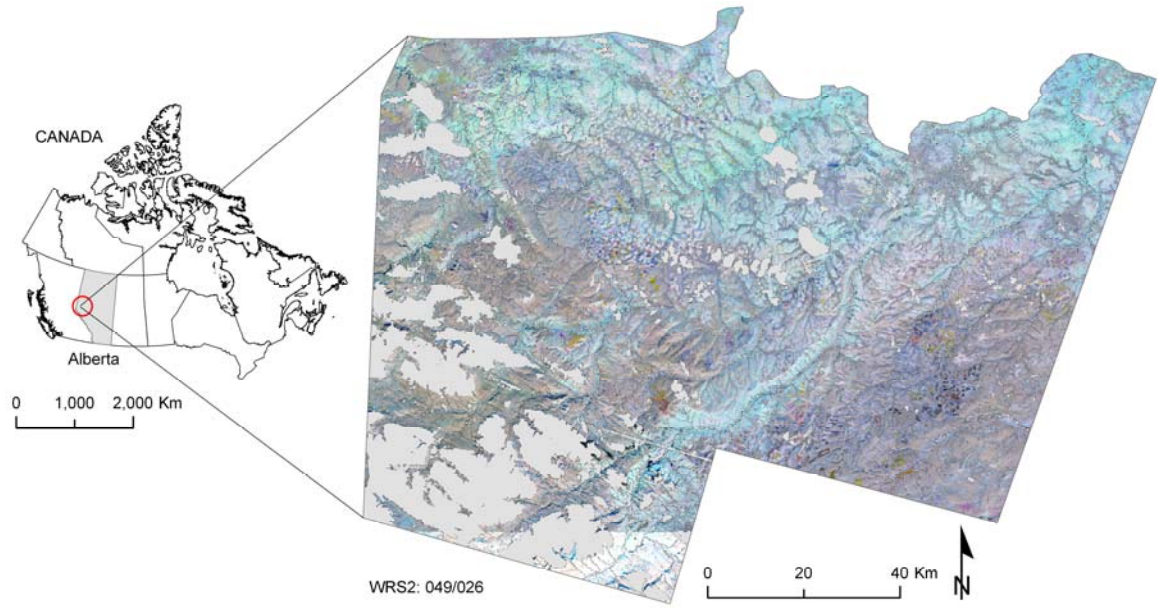

Figure 1. Location of the study area. The inset displays a combination of Tasseled Cap Angle (TCA) layers of years 2001 (Red), 2002 (Green), 2004 (Blue); areas of clouds and altitude over 1700 m are masked out.

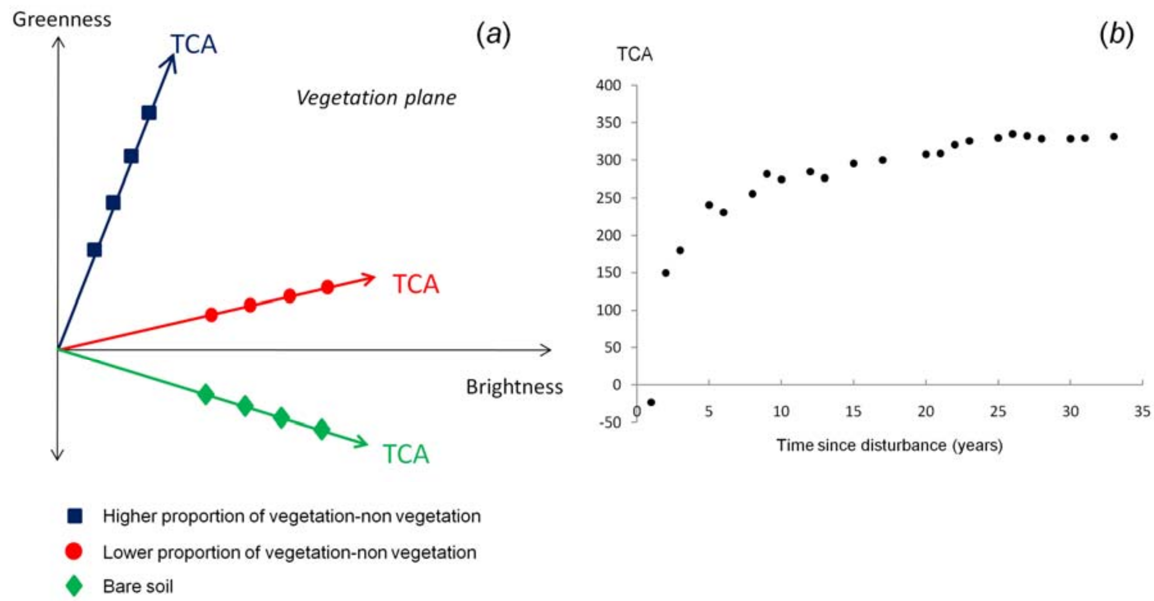

Figure 2. (a) Tasseled Cap Transformation Brightness and Greenness components form the vegetation plane (Crist and Cicone, 1984). The TCA is the arc tangent formed by Greenness and Brightness. Forest stands with higher proportion of vegetation-non vegetation show higher values of TCA, bare soil shows negative TCA. (b) TCA average values of disturbed areas in the study area in the last 35 years; recent clearcuts show negative TCA value.

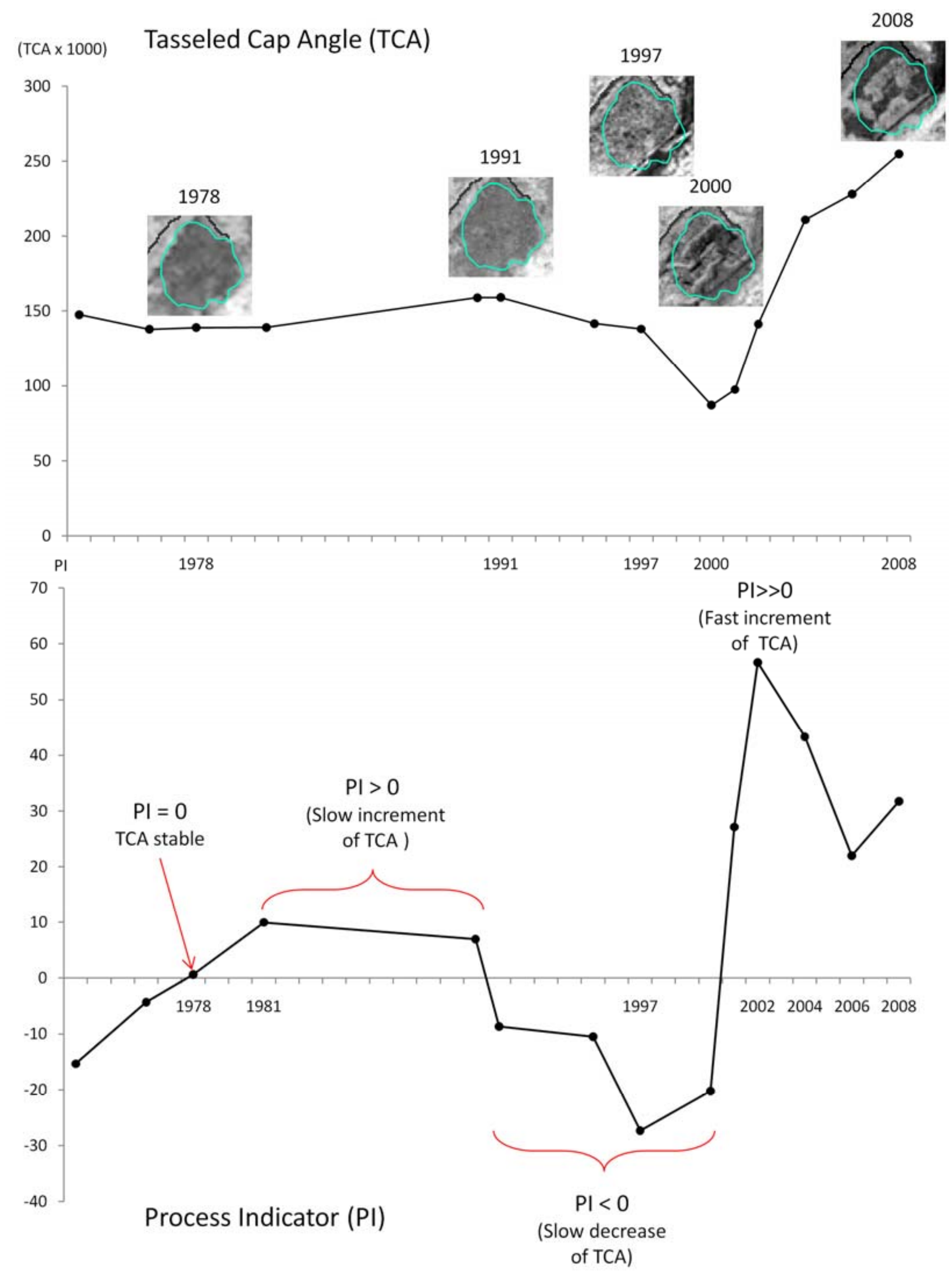

Figure 3. TCA (1973-2008) and PI (1976-2006) trajectories of a L1 object. The PI is calculated as the derivative of the TCA curve (interpolated with a second order Lagrange polynomial). PI values correspond to each date.

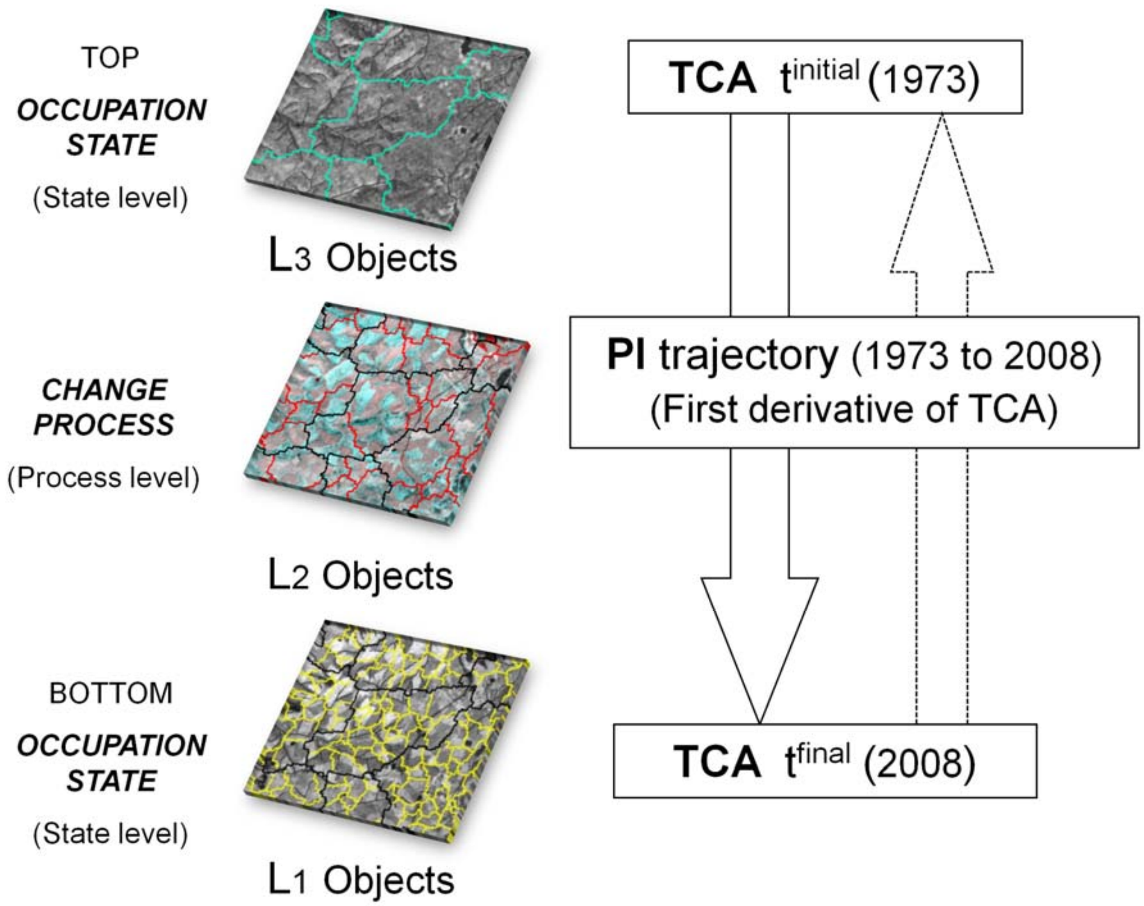

Figure 4. Hierarchical spatio-temporal segmentation process. Bottom level 1 of homogeneous actual occupation states objects serves as base for creation of top level 3 representing homogeneous occupation state objects at initial date. Objects of intermediate process level are limited in size and boundaries by both occupation state levels.

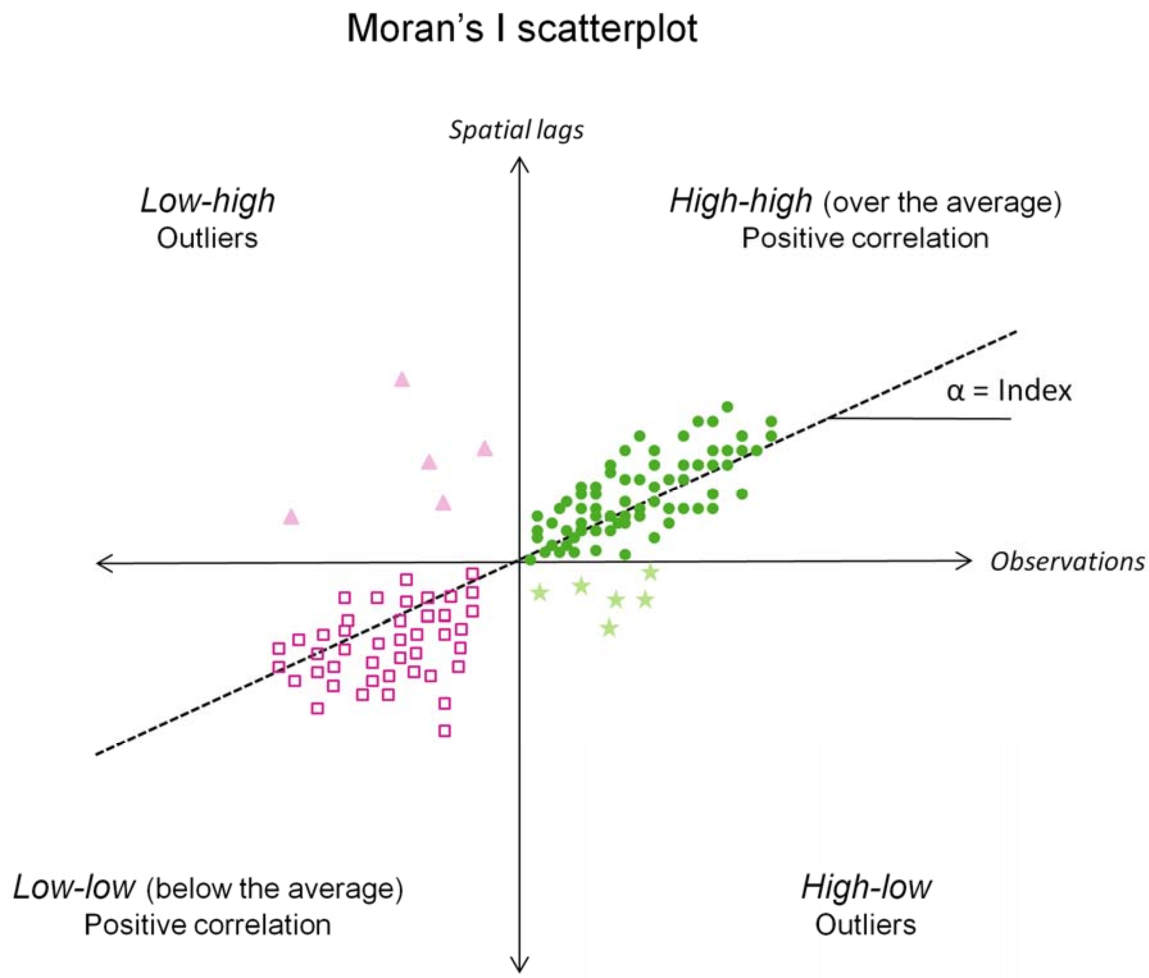

Figure 5. Moran's I scatterplot. The slope of the regression line is an estimation of the global Moran's I. Relative density of points in the correlation quadrants indicates how the global measure of spatial association is determined by association between high or low values.

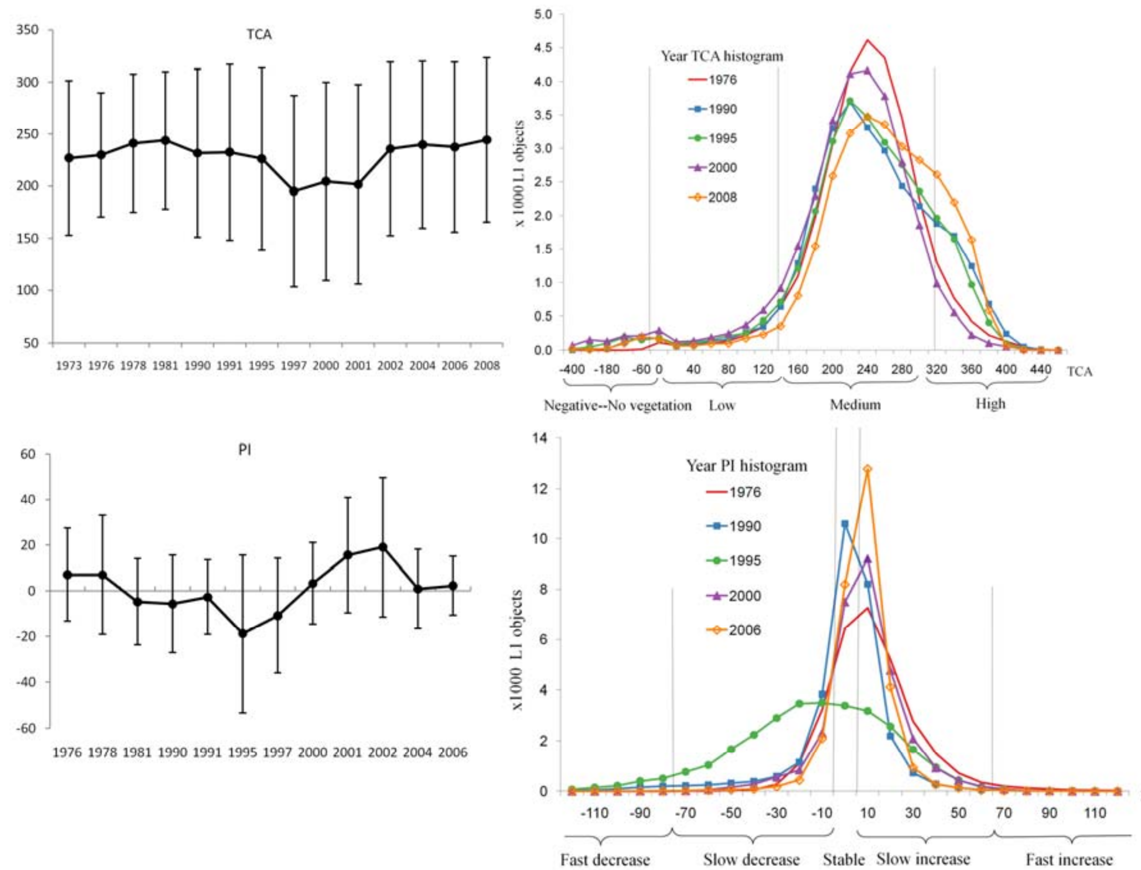

Figure 6. Mean ± 1 standard deviation of TCA values of L1 objects (other object levels show similar trends) (left). Histograms of TCA and PI distribution (right).

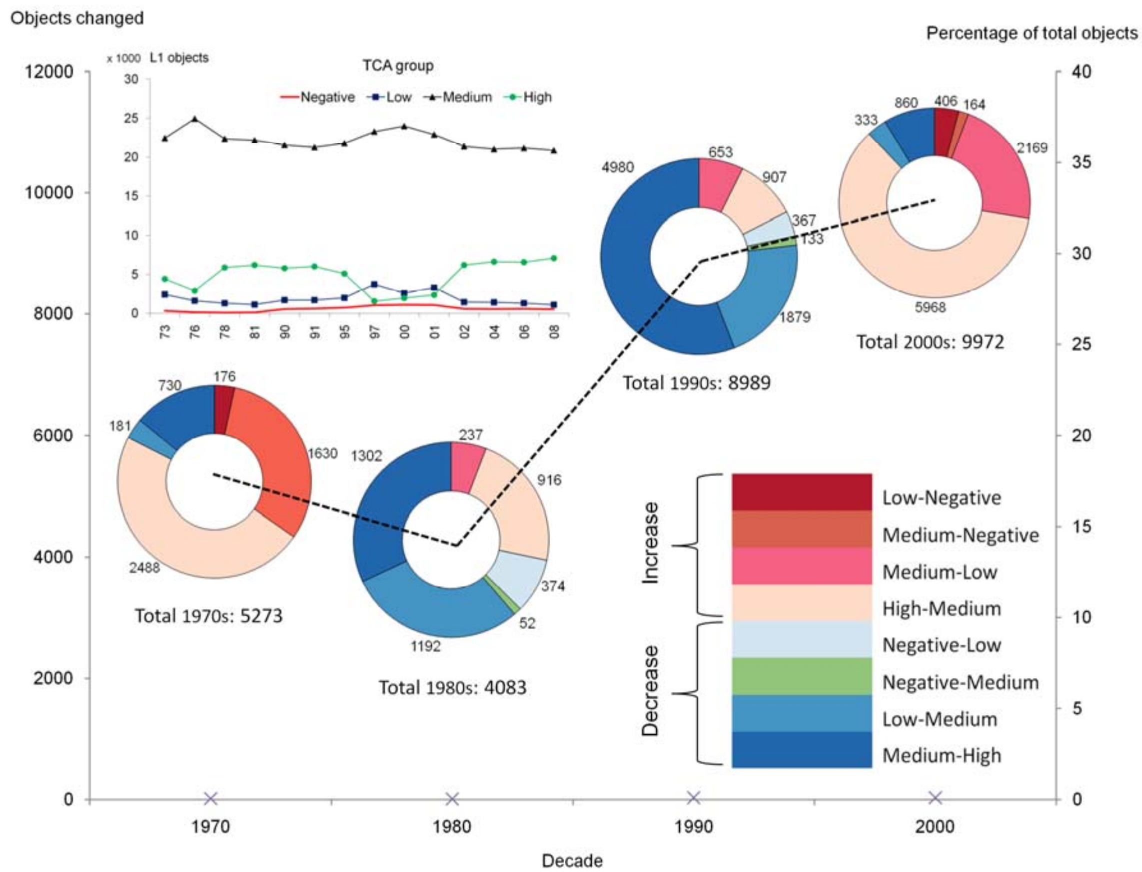

Figure 7. Changing objects between TCA categories in each of the last four decades. Evolution of total number of objects in different TCA groups at level 1 (top left inset) (other levels of segmentation show similar trend).

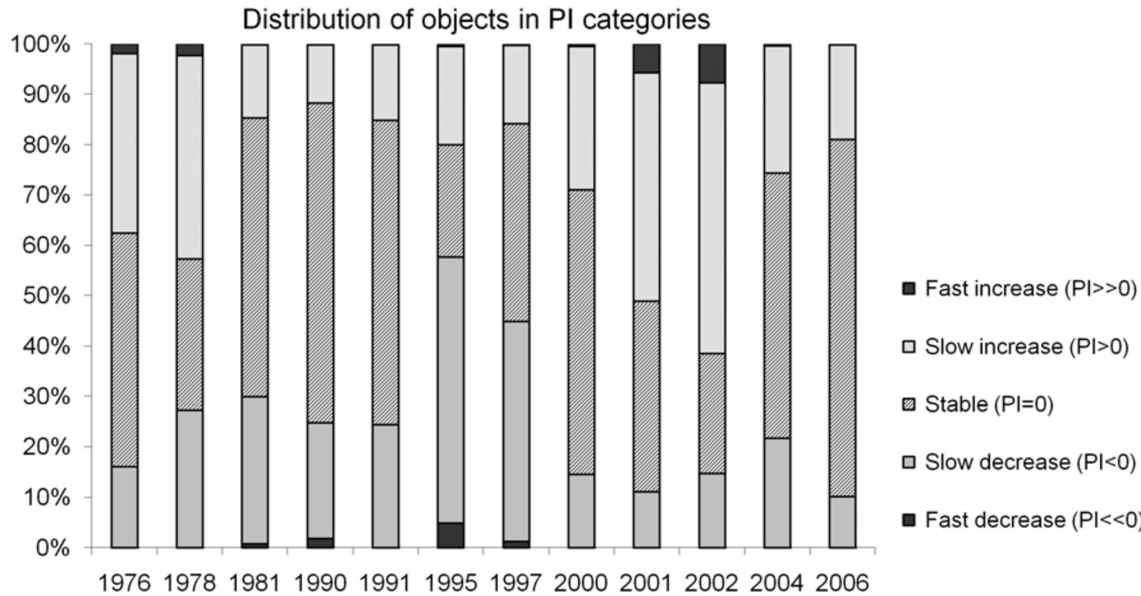

Figure 8. Evolution of change process (PI) categories of level 1 objects.

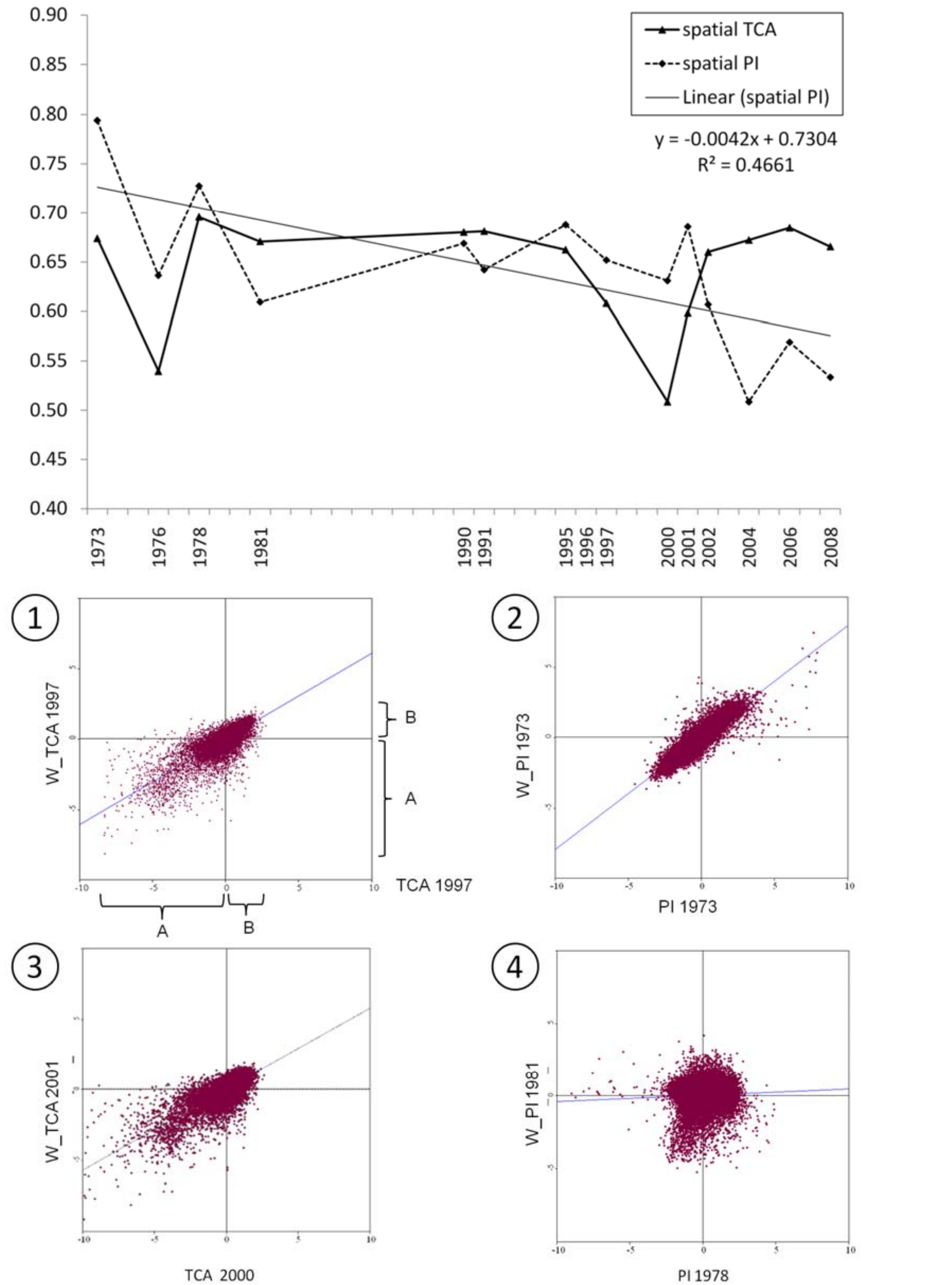

Figure 9. TCA and PI spatial global Moran's I trends (top). Spatial (univariate: 1, 2) and temporal (bivariate: 3, 4) Moran's I scatterplots of TCA and PI (bottom)

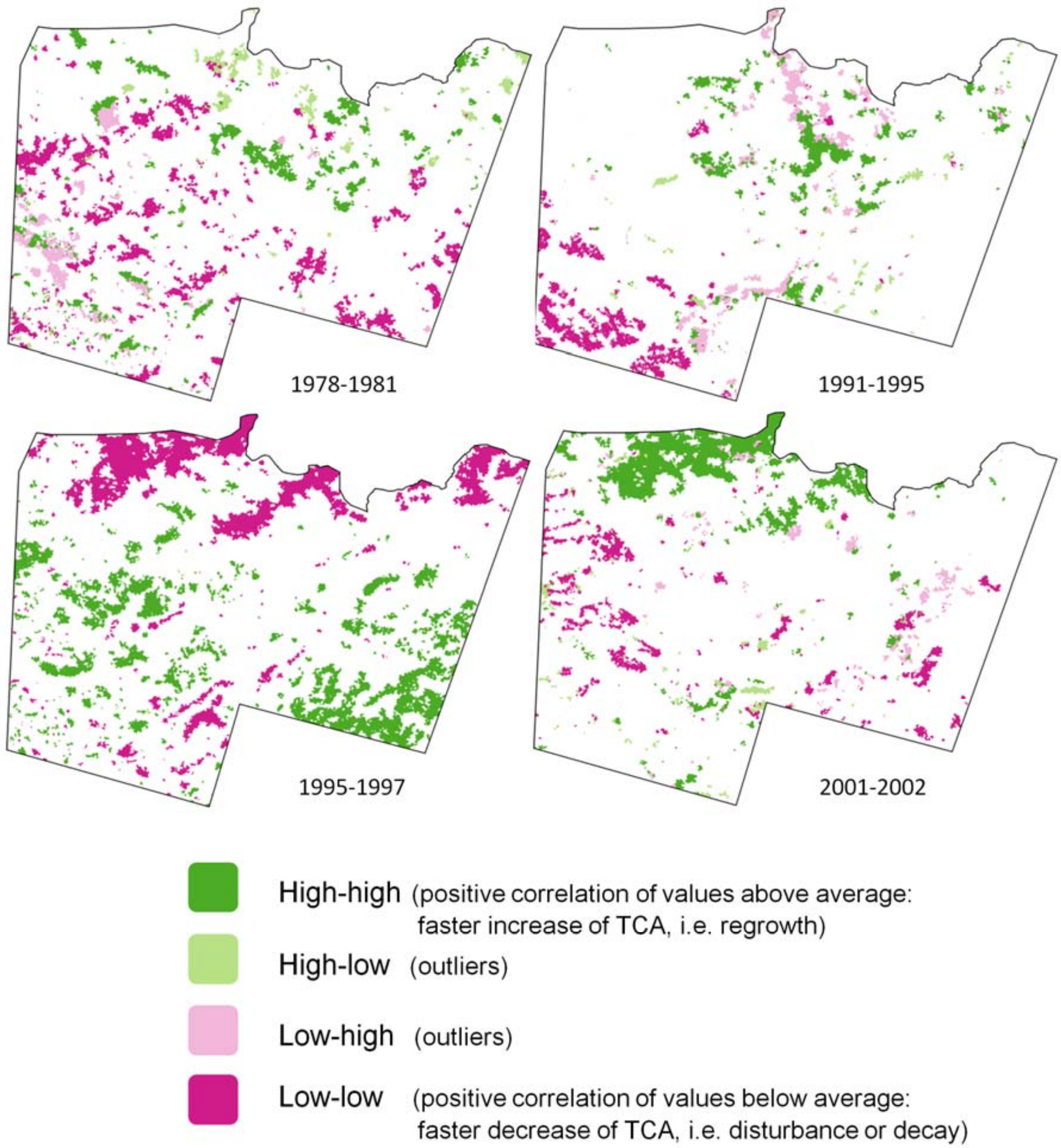

Figure 10. LISA Maps of temporal association PI clusters; only significant polygons (p<0.01) are colored.

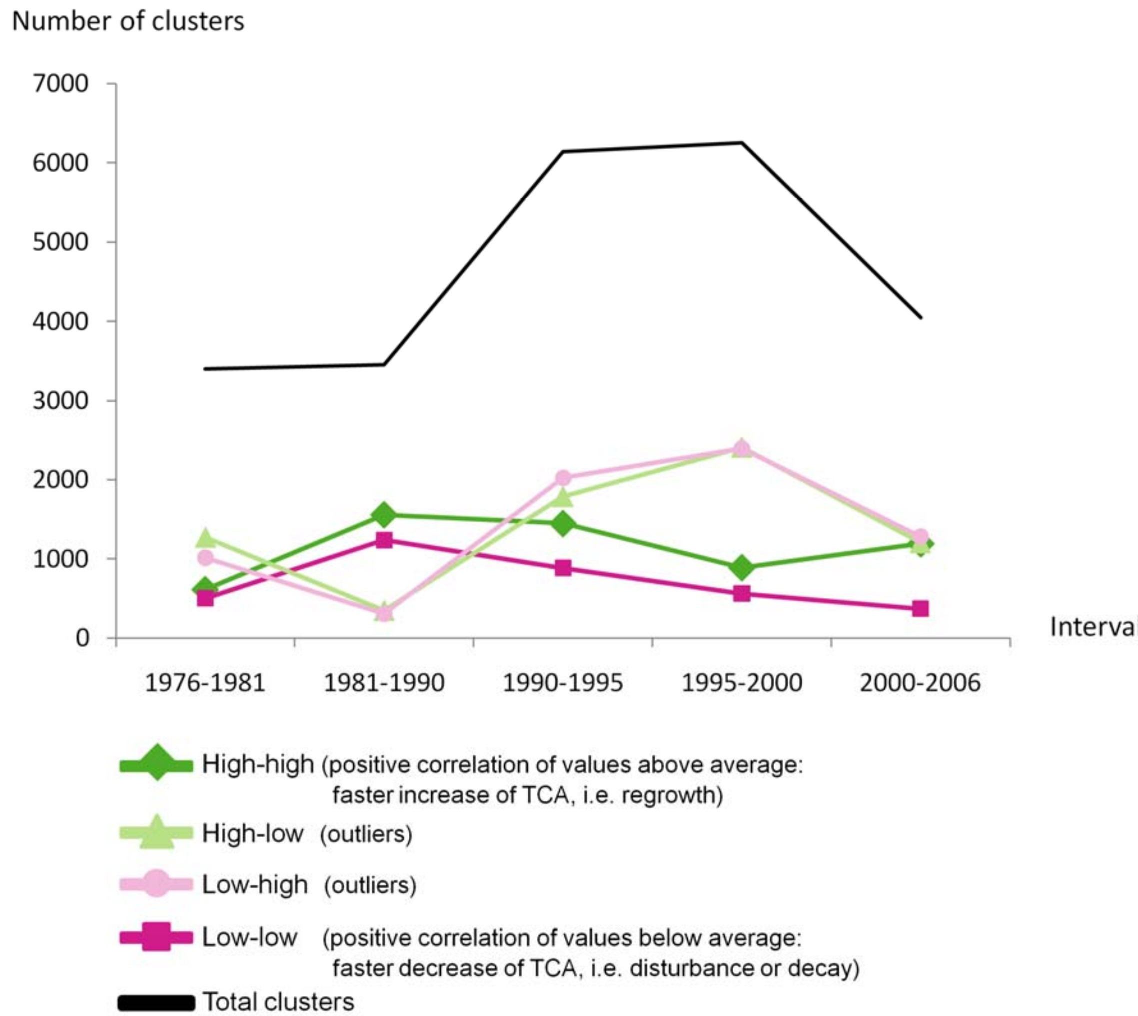

Figure 11. Evolution of significant clusters per quasi-quinquennial period

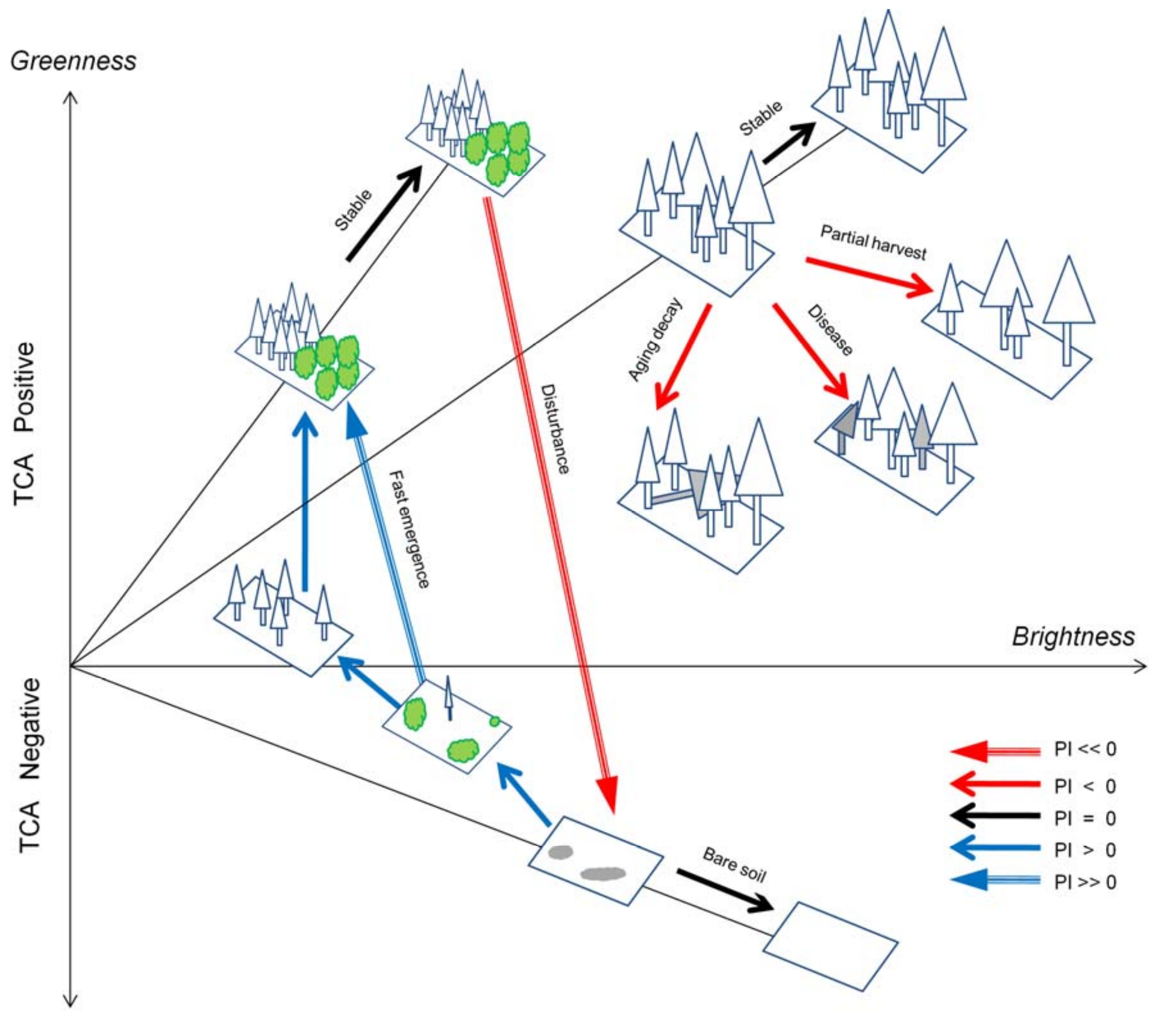

Figure 12. Relative TCA values of various occupation states of the coniferous forest in the study area and PI values of changing processes.